The authors would like to thank the reviewer for his/her valuable comments which helped improving the quality of the manuscript. Our point-by-point responses to the reviewer's comments appear in bold below.

Reviewer 1

1. Use of an acronym "ATR-42" in the first sentence of the abstract is not helpful for those who do not know what ATR-42 is. Perhaps "manned research flights" ? Use of the ATR-42 is jargon. I did not know which aircraft it is. Perhaps describe the aircraft in the paper and call it ART-42 thereafter.

"ATR-42" has been replaced by "manned research flights".

2. Line 6: I understand the desire to write a catchy first sentence, but "radiator fins" on traditional "radiators" don't accomplish their purpose through radiation. They actually transfer thermal energy from one substance (a circulating fluid or highly conductive metal) to the air around them through conduction at the interface of the fin and the air that is it immersed within and not so much radiative losses. (Note: most traditional radiator fins are made of shiny metal that have less than ideal emissivity making them poor radiators anyway.) Then, after the air around the fin is warmed, it is transported away either through forced movement or natural convection. The exception are radiator panels on spacecraft that function as the authors are suggesting clouds do, but they are a rare form of embodiment of radiators and actually look like large flat panels and not fins that you find on common devices. So, I understand the author's ambition to convey the importance of clouds in the upper atmosphere, but the current way it is written is not a good analogy and worse could lead an uninformed reader to the wrong idea about how most radiator fins work.

"Subtropical regions have long been considered as the radiator fins of the Earth due to their dry free troposphere and their ability to emit a large amount of heat to space (Pierrehumbert, 1995)."

Has been replaced by

"Subtropical regions play a major role in the radiation balance of the Earth due to their dry free troposphere and their ability to emit a large amount of heat to space (Pierrehumbert, 1995)."

3. The very first sentence of the paper is also interesting because my elementary textbook understanding of the global energy budget is that the low latitudes cannot cool enough via radiation and that surplus energy is transported poleward through large scale circulations. In contrast, the high latitudes experience a deficit in the radiation budget because loss of radiation prevails over incoming radiation. (See Fig. 17 in Ahrens "Meteorology Today")

The emission of LW radiation to space is obviously not the only way through which the energy balance of the atmosphere is achieved, but it is a major ingredient of it.

So, what is it about the subtropics (roughly 10 – 30 degrees latitudes) that makes them special in terms of their ability to radiate energy? Again, this is in regard to the very first sentence of the paper.

Barbados is located at 13N. In Summer, it can be associated with deep convection from time to time, but most of the time, and certainly during the whole winter season, it is

associated with large-scale subsidence and very dry conditions in the free troposphere (in winter, it is frequent to find relative humidities of 3-5% over the whole free troposphere!). These dry conditions in the free troposphere and the prominence of clouds in the boundary layer (as opposed to deep convective clouds) make the area of Barbados representative of the trade-wind regimes of the tropics. As a matter of fact, the clouds around Barbados have been shown to be representative of the cloudiness of the trade-wind regions of the globe (Medeiros and Nuijens, PNAS, 2016). The Barbados area thus contributes to the strong emission of LW radiation at the top of the atmosphere (the low humidity and rare upper-level cloudiness entail a strong infrared cooling to space) that plays such an important role for the radiation balance of the Earth. Indeed, the moist areas associated with deep convection are too radiatively opaque to get rid of their energy excess through radiation; it is largely done through a redistribution of energy by the Hadley-Walker circulation which induces subsidence in the subtropics and thus allow energy to be emitted to space through infrared radiation (the origin of the 'radiator fins' expression of Pierrehumbert 1995). The effect of subtropical LW emission on the net tropical radiation budget is already taken into account in the figure shown by this Reviewer; if it wasn't, the energy excess in the tropical belt would be much higher, and the large-scale atmospheric and oceanic circulations would need to be much stronger to balance it.

Several factors make the trade-wind regimes 'special' regarding their ability to radiate infrared radiation to space. First these regimes cover a large fractional area of the tropical belt, and thus have a huge statistical weight, making them highly susceptible to influence the tropical radiation budget. Actually, this is the primary reason why trade-wind clouds are so critical for climate sensitivity. Second, as discussed above, they emit much more infrared radiation than the moister deep convective regions. Third, because of the low IR opacity of the free troposphere in these regions, the infrared radiative cooling is very strong at the top of the boundary layer, which has the potential to generate radiatively-driven mesoscale circulations within the boundary layer and can contribute to organize the low-level cloudiness.

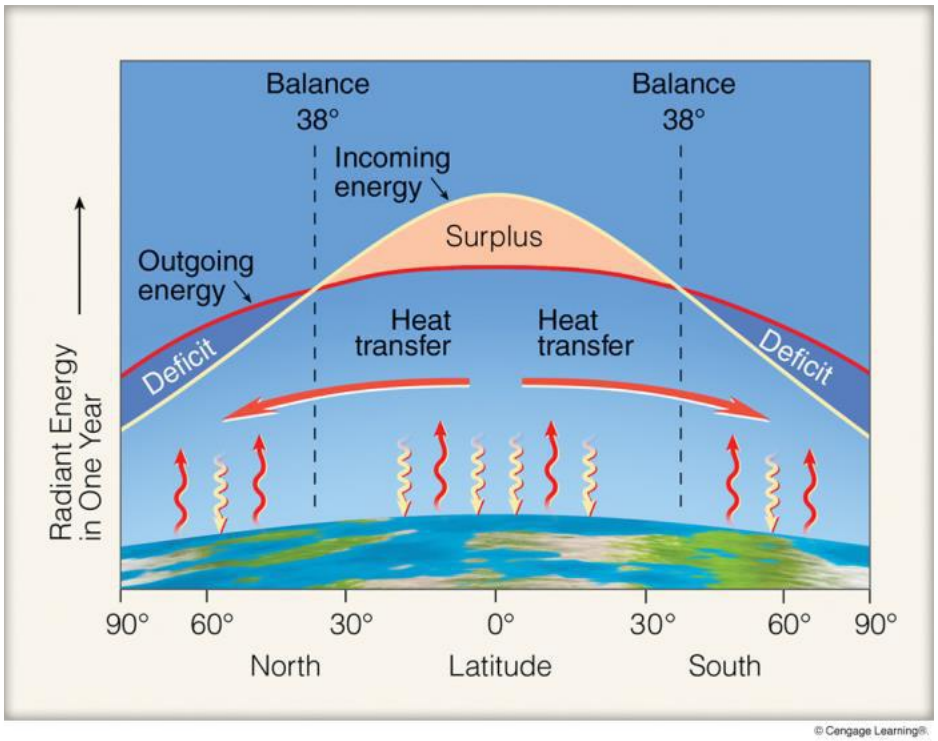

4. Line 7: Try to avoid referring to heat as a noun. What is heat? It is ambiguous. Some people regard radiation as heat. Some regard anything having temperature as heat. Yet these are very different forms of energy. More precise language helps avoid confusion. (Read Bohren & Albrecht, Atmospheric Thermodynamics, 1998, pages 24 – 28.)

Here, we are talking about heat in the thermodynamic sense, we are talking about the heat (in J) released by the Earth system through radiation (radiative fluxes correspond to heat fluxes, in W/m2).

5. Line 9: "contribute to cool the Earth further" is awkward wording. Perhaps "contribute to further cooling of the Earth…"

"contribute to cool the Earth further…" has been replaced by "contribute to cool the Earth…"

6. Line 1 on page 2: "lidars have the potential to detect them much better" is a broad-brush statement that may not in fact always be true. The first part of that sentence was about passive sensors and but lidars are active sensors. I think one should not belittle passive sensors because lidars also have limitations where radiometers excel. Just carefully point out what lidars can do that passive sensors cannot. That is fair. But don't be dismissive of all passive sensors in half a sentence.

We are not dismissive of the passive sensors we routinely use for our scientific work. We are well aware of their limitations, such as the advantages and disadvantages of lidars. It remains true that lidars detect clouds better (at least their cloud top for lidars in space, or cloud base for lidars on ground) when the cloud layers are not overlapped or masked by thick clouds. In the latter case, their detection from passive sensors can be also difficult.

In contrast, under certain conditions lidars have the potential to detect them much better (Liou and Schotland, 1971; Spinhirne et al., 1982).

7. Page 3, Line 25, “shooting”? Like with a gun? Perhaps “projection” is more appropriate for a laser or lidar?

The term "shooting" is often used as for example in J. N. Porter; B. Lienert; Shiv K. Sharma J. Atmos. Oceanic Technol. (2000) “In order to derive the aerosol scattering coefficient […] we have implemented a simple forward stepping algorithm with a modified horizontal shot technique."

8. Page 3, line 24-25: how does one know whether the atmosphere is homogeneous? What constitutes sufficient homogeneity?

This is discussed in section 5.3.2. A reference has been added (Chazette et al., 2007).

9. Lines 32 and 33: use of the word “the” too many times.

The correction has been done:

"The goal of this paper is to present the flight strategy, ~~the~~ measurements, ~~the~~ data processing and ~~the~~ cloud and aerosol products derived from the horizontal lidar measurements made during the EUREC4A campaign."

10. Line 1 on page 4: comma not needed before the word and

The correction has been done:

"Section 2 presents the ALiAS lidar characteristics~~,~~ and Section 3…"

11. Line 8 on page 4: Acronym LSCE was not defined in the body of the paper.

The acronym has been defined:

"LSCE (Laboratoire des Sciences du Climat et de l'Environnement)"

12. Line 11 on page 4: wavelength is not the only issue that makes it eye-safe. The pulse energy, rep rate, and beam diameter also contribute. I suggest stating that eye-safety is a result of all of these parameters. It would be helpful to cite a document that explains in detail the eye-safety calculation.

The sentence has been modified as:

"…emitting at the wavelength of 355 nm. It satisfies eye safety requirements (EN60825-1) at the output window considering the characteristics given in Table 1 (emitted wavelength, pulse energy, repetition rate, beam diameter and pulse duration)."

13. Line 12 on page 4: Is the use of PXI architecture really worth mentioning? Is it related to the performance of the lidar? Why mention it here? For me, what is much more important (and not clear) is the next point:

Yes, this is important to mention because it is a stable technology, specifically suited for airborne experiments. This type of computer is robust to the temperature excursions that can take place in an airplane cabin while flying in the tropics.

14. Page 4 or 5: The paper does not mention the specific detector used. Table 1 lists analogue detection but also indicates a photomultipler (PMT) is used. Aren't PMT digital detection as in photon counting? I suggest being more specific on what detector (please state make and model) and what sampling electronics (make and model) are used. These are critical to understanding the nature of the backscatter data.

The detection is analog as written in Table 1. The detectors are photomultipliers as also indicated in Table 1, they are from the Hamamatsu company, the model is Hamamatsu H10721P-210. They provide an analog signal that is acquired as is by a PXI-5124 fast digitizer working at 200 MHz and 12 bits, without going through a pulse (photon) counter.

This information has been added in the text and in Table 1:

"The acquisition system is based on a PXI-5124 (PCI eXtensions for Instrumentation) fast digitizer working at 200 MHz and 12 bits, without going through a pulse (photon) counter leading to…"

Wavelength	**355 nm**
Pulse repetition rate	**20 Hz**
Pulse duration	**8 ns**
Beam diameter	**25 mm**
Divergence	**<0.2 mrad**
Reception diameter	**150 mm**
Filter bandwidth	**0.2 nm**
Field of view	**3 mrad**
Detector	**Photomultiplier**
Detection mode	**Analogue**
Digitalization	**12 bits**
Native line of sight resolution	**0.75 m**
Dimensions of the optical head	**45 cm (height) 28 cm (width) 18 cm (deep)**
Weight of the optical head	**~15 kg**
Weight of the electronics	**~20 kg**
Power supply	**220 V AC**
Consumption	**<500 W**

15. Line 5 on page 5: How about: "ALiAS was installed in the aft of the ATR-5 42 aircraft in an orientation that enabled a direct near-horizontal line-of-sight." (Use of the word direct indicates that no scanner was required to achieve this. Near is the truth. It is not always perfectly horizontal.) You may include a sentence that there was no effort to steer the beam to maintain horizontal pointing and compensate for aircraft attitude.

Agreed, we have modified the sentence as:

"ALiAS was installed in the aft of the ATR-42 aircraft in an orientation that enabled a direct near-horizontal line-of-sight."

16. Line 19. Could "right" be replaced with something more specific like "starboard"?

" …back of the ATR-42 aircraft, on the right side."

has been replaced by:

"…back of the ATR-42 aircraft, on the starboard side."

17. Line 23 page 6: what does prototypical mean here? Was it the actual flight or the flight plan? The first of two per day? Maybe prototypical is not the right word choice.

"prototypical flight plan" has been replaced by "flight strategy".

18. Line 23 on page 6 to line 3 on page 7. This is one huge sentence that does not read well. I recommend breaking it up.

"It was built along 5 major phases (see Table 2), each of which was designed to address a particular lidar-related science needs, and requirements of the lidar and other remote sensing and in situ instruments composing the ATR-42 payload (radar, aerosol and cloud microphysics, water vapour stable isotopes using cavity ring-down spectrometry, turbulence), while contributing to the multi-aircraft and statistical sampling strategy implemented during the field campaign:"

has been modified as:

" The flight strategy is given in Figure 3 for the flight on 26 January 2020. It was built along 5 major phases (see Table 2), which contributed to the multi-aircraft and statistical sampling strategy implemented during the field campaign. Note that during straight-line flights, the typical speed of the aircraft was ~100 ms-1. Each phase was designed to address particular scientific requirements of the lidar and other remote sensing and in situ instruments composing the ATR-42 payload (radar, aerosol and cloud microphysics, water vapour stable isotopes using cavity ring-down spectrometry, turbulence):"

19. Line 25 on page 6: what is a "lidar-related science needs" ? This is a vague phrase and leaves the reader wondering. I think the word "needs" should be singular (need) and not plural.

Agreed. Resolved with previous response.

20. Line 7 on page 7: I suggest "Such an aircraft sounding was aimed at…"

" Such aircraft sounding aimed at…" has been replaced by "Such an aircraft sounding was aimed at…".

21. Line 8 on page 7: Please clarify whether "retrieving aerosol extinction coefficient and volume depolarization ratio profiles" was done using in situ sensors or the lidar. I think this requires a much more explanation and references.

It is done with the lidar. Information and references are given in section 5.3.2. The sentence has been revised as

"Such aircraft sounding aimed at retrieving aerosol extinction coefficient and volume depolarization ratio profiles from the lidar measurements (see subsection 5.3.2) and…"

22. Line 10 and 11 on page 7: If it is worth noting then why not tell the poor reader the dates and times? Why tease them? Maybe a footnote or a reference to where they can find these cases?

Reference was made to subsection 5.3.2 where this is presented.

23. Line 25 on page 7: “Lower troposphere” is pretty general and not helpful. Can you be more specific? In or out of the boundary layer? At the top of the convective boundary layer? Were you flying through the entrainment zone (EZ)? Above the EZ? Perhaps in the capping inversion?

" …performed in the lower troposphere, at CBH,…" has been replaced by "performed at CBH…"

24. By the way, flying in the entrainment zone is typically pretty bumpy ride and the atmosphere is not very horizontally homogeneous (a horizontal lidar beam penetrates inversion air and BL air in plumes). This is challenges two requirements for this project: (1) minimal rolling to maintain horizontal probing and (2) horizontal homogeneity. So, if the flights were indeed near the top of the BL (just above cloud base) near the EZ, can you please comment on whether these issues challenged the measurement goal?

In fact, the measurement goals have not been affected. The ride turned out to be rather smooth, which we could experience directly by flying on board with the lidar. The variations in the attitude of the aircraft did not induce a deviation in the horizontal of the lidar line of sight of more than 1±0.5° (measured at all times by an inclinometer along a straight route). In addition, there is a quality indicator given in 5.3.1.c.

We have added in Section 3 the sentence:

"Its orientation was measured at all time by an inclinometer."

We have added the mean value and the standard deviation of the angle of the lidar line of sight with the horizontal in subsection 5.3.1.a:

" …(the mean value is 1° and the standard deviation is 0.5°)."

25. Lines 8 – 9 on page 8: breaking the sentence across two points like this is not good style. Complete a sentence and start a new sentence.

We have modified as:

"4. …lower part of the boundary layer.

5. The ATR-42 cruised back towards Barbados around 3 km a.m.s.l. (see Figure 3)."

26. Line 13 page 8: use of prototypical again. (See point 17 above.) I understand a prototype is a first version of something but in this case the question is whether the first version was actually flown or was the long description just an ideal plan that was never actually done.

We have replaced by:

" The flight strategy "

27. Line 7 page 9: Use of the word “onwards” not needed because there is no level above 3.

"For level 3 onwards that they are considered globally by flight segment to establish statistics."

has been replaced by:

" The statistics performed on Level-2 data are gathered in the Level-3 data. Statistics are computed for all flights for the aerosol Level-3 products and for the Phase 2 of the flights for the cloud products."

28. Line 7 – 8 page 9: I really don't know what this means: "For level 3 onwards that they are considered globally by flight segment to establish statistics." What does "considered globally by flight segment" mean?

Agreed, we clarified by replacing the sentence. See previous answer.

29. Line 1 on page 10: The sentence "This section presents the physics of the measurement." should be removed. "…the physics of the measurement" is a huge and complex topic that would require several books to fully explain. Surely the manuscript is not covering all of it in this section. Maybe "This section presents the steps taken to derive data products."

Thank you for the suggestion, we have replaced " This section presents the physics of the measurement." by "This section presents the steps taken to derive data products."

30. Figure 4. This figure looks nice but I find it not very helpful because it is vague. For example, the following part of the figure is confusing. Are some arrow heads missing? It is not clear what is informing what. Where does "aerosol extinction coefficient direct calculation in cloudless situations" come from? Lidar data? What level?

The Figure 4

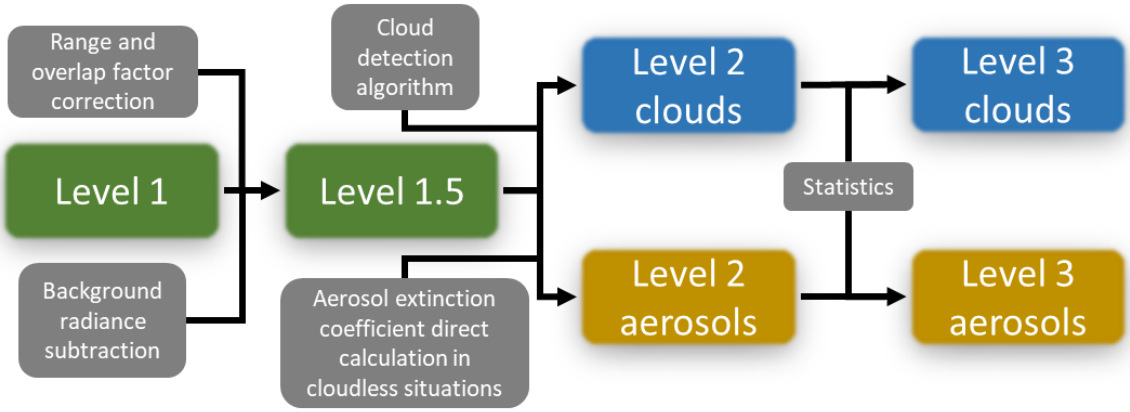

has been replaced by

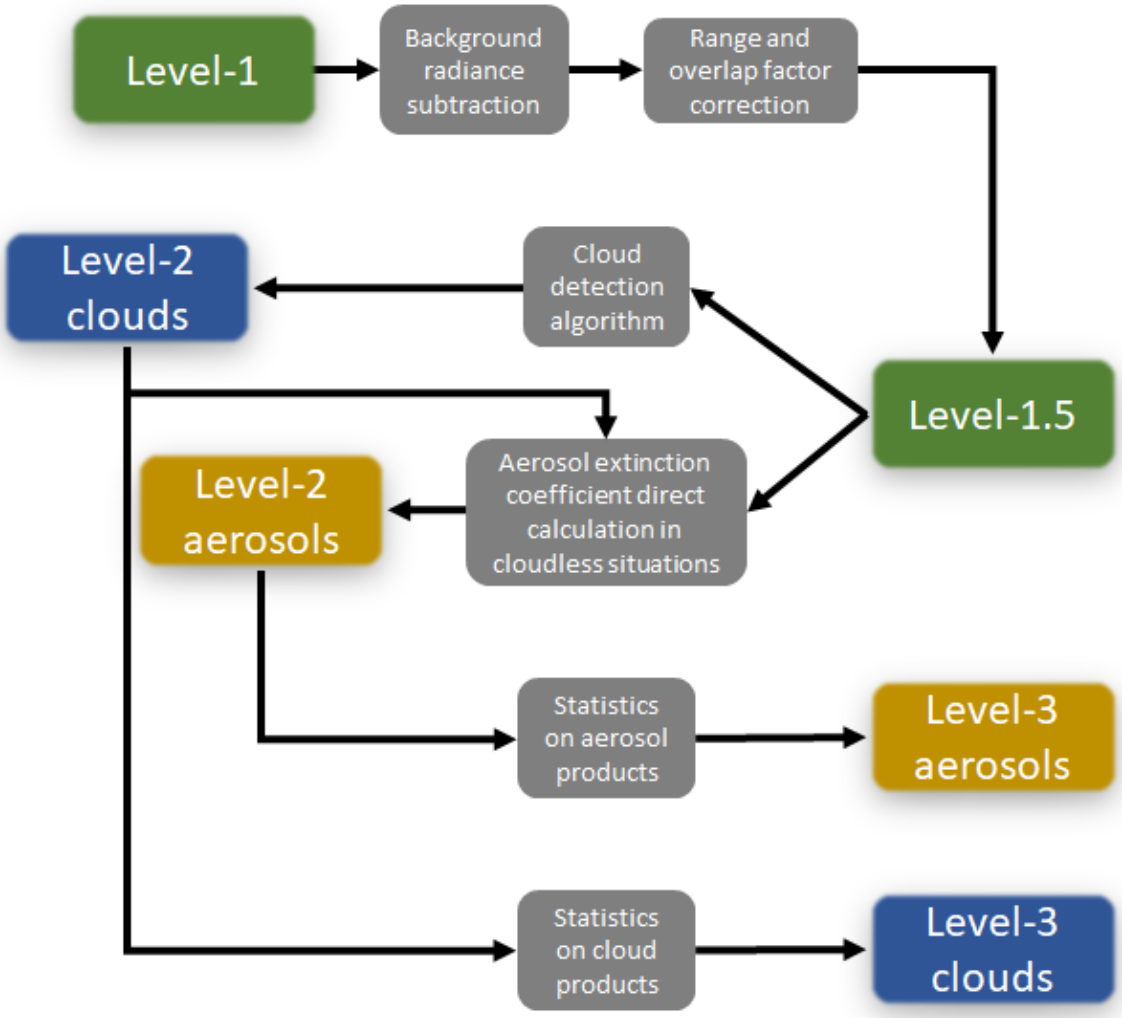

31. Line 12 page 10: Volts should not be capitalized.

The correction has been done.

32. Line 12 page 10: Who cares whether they are in volts or digitizer counts? Isn't the voltage of backscatter data arbitrary? Really, why is data in volts important to note? Why is it in volts especially considering it uses a PMT? Shouldn't they be in counts?

It is not particularly important for the processing, but the detection is performed in analog and we record volts. It is the unit of the level 1 data. As explained in a previous response (reply to comment #14), there is no photon counting. The choice of analog is necessary to avoid saturation of the counting mode because of the strong signal, due to daylight and the presence of clouds that may be close to the lidar during flights.

33. Line 13 page 10. Resolution implies the ability to resolve. Given that the pulse length is 8 ns, I doubt you could distinguish two independent aerosol features that are 0.75 m apart. Perhaps the word "resolution" is a bit misleading. It is really more like spatial sampling along the beam. Whether those are truly independent samples or not is another question. It depends on the response time of the detector and amplifier. One could have 500 MHz sampling, but it doesn't provide value if the pulse length is long and the electronics are slow.

Indeed, and that is why we talk about “native” resolution, i.e. sampling rate. To ensure independence between each point of the profile, the signal is sub-sampled before analysis and the resolution along the line of sight is then 15 m. A sentence is missing in subsection 1.5 to explain this part, it was added as:

"To build level 1.5 data, the raw sampling along the line of sight has been degraded in order to ensure the independence of each point on the horizontal lidar profile. The final resolution is then 15 m. The ALiAS-derived level 1.5 data are then profiles corrected…"

34. Bottom of page 10. Just wondering: How many bits of dynamic range is in the detection subsystem on this analogue lidar? (Again, I am confused because Table 1 indicates it uses a PMT which tells me it is photon counting but it also lists analogue detection mode. What am I missing?) If it is analog detection, then the number of bits is important to understand how well resolved the dynamic range is.

It is possible to do analog detection with a PM, it is recommended in the UV/visible spectrum. Then, there is necessarily a digitization which is carried out. It is here on 12 bits. The digitalization noise is therefore negligible here. The number of bits has been added in Table 1. See remark 14.

35. Line 18 on page 11. I suggest replacing the word “verified” with “true”.

The correction has been done:

"…the heterogeneity is too strong for this hypothesis to be true."

36. Figure 5. Congratulations on achieving a flat background. However, many people who use this data will wonder why a description of this exercise is in the paper especially if it is not a problem. As having practiced lidar development I appreciate it and think it is worth keeping. But others will wonder. So, I think it would be helpful if the manuscript stated why this was investigated and why you bother to show it. Perhaps cite some examples where it was a problem? Without a good explanation, some may think it is just filler to fatten up the paper with technical stuff.

We have clarified the interest of this figure:

The sentence:

" From level 1 data, the eventual shift of the lidar signal baseline is checked for each flight in order not to introduce any bias during data processing, mainly in the far field, i.e. beyond 4-5 km."

has been replaced by

"Baseline distortion can significantly increase the rates of non-detection and/or false detection of cloud structures. Hence, in Level-1 data, potential drifts of the lidar signal baseline are checked for each flight, in order not to introduce any bias during data processing, mainly in the far field (i.e. beyond 4-5 km)."

37. Isn’t a plot of a single waveform for level 1 data more important than a scatter plot showing the flat baseline? (Just wondering why there is not a figure to show a typical return from 1 pulse of level 1 data.)

After years of practice, we consider that a scatter plot allows providing more robust data verification on the dependency of the baseline drift on the sky background level, as well as helps visually averaging out noisy data. In addition, a typical return is given as an example in Figure 10.

38. How much averaging (temporal or spatial) is ever done to the data. I don't recall reading anything above smoothing and it might be worth pointing this out,

Agreed, we have modified the sentence:

"The native resolution of the lidar profiles is therefore 0.75 m along the line of sight."

by

"The raw sampling of the lidar profiles is 0.75 m along the line of sight and an average over 50 shots is performed during the acquisition, corresponding to about one recording every 5 s (2.5 s averaging time and 2.5 s recording time)."

39. Same question as above for level 1.5 data. Why not make a plot that shows how data processing transforms a given waveform from level 1 to level 1.5? Then people can see a plot of the actual data. This is helpful so that when they read the data they can check to make sure they see the same thing. They can attempt to recreate the plot on their own and be sure they are looking at things correctly.

This kind of plot is not very graphical because of the difficulties to find an adapted scale when correcting for the solid angle. As seen in remark #33, only the resolution along the line of sight is degraded at 15 m. The temporal resolution remains unchanged.

40. In fact, I am thinking of a plot that shows the progression of going from level 1 to level 1.5 etc all the wave up to the final product: cloud boundaries. That would be nice.

We already have some of this in Figure 10. There is not really much interest in showing raw data profiles, it is more the ABC that is interesting (solid angle correction).

41. Figure 6 panel b shows the "apparent backscatter coefficient" close to the aircraft (< 1 km range) tend to be more orange than the data out at 2 or 3 km which tends to be yellow. Is this the result of attenuation that is not corrected? I think it is worth explaining this in the manuscript.

The apparent backscatter coefficient is corrected for the molecular transmission, but not for the aerosol and cloud transmission as shown in Equation (3).

Indeed, it becomes more yellow away from the plane because of attenuation by aerosols and clouds.

We have added the sentence:

"The ABC decreases away from the plane because of attenuation by aerosols and clouds (passing from orange to green on Figure 6a)."

42. Please state (it may require a new paragraph) the distribution of roll angles during a typical flight leg and the implications of aircraft roll on the altitude of the lidar beam as a function of range. For example, what happens to the altitude of the beam at 8 km range if the aircraft rolls off of perfectly a horizontal plane by 1 degree? Perhaps the flight data could be used to mark

each range gate in a lidar return with an estimated altitude. Also, can the authors please comment on the implications of variability in aircraft roll on what this means for the cloud location data? Is it possible that at one moment the lidar beam intercepts a small cloud but the next moment it misses the cloud because the aircraft rolled a little bit? Could this rolling (due to the turbulence) make the cloud results look less coherent and more noisy?

The effect of roll is taken into account in the quality indicator/flag. As explained above it is less than 1±0.5° during Phase 2 (subsection 5.3.1.c). We have considered it because indeed we can miss small clouds at great distance.

The Qflag parameter in Table 4 (subsection 5.3.1.c) contains this information via the vertical positioning with respect to the horizontal (Δz).

43. Line 8 and 9 of page 28: what means “altitude parameters”? This is vague. Is it altitude of the aircraft for each pulse? Is it altitude of the beam for each range gate?

Agreed, we have modified as

" flight attitude, localization and altitude".

44. Section 5.2.2: Many non-lidar scientists will not understand what overlap factor is. Perhaps one or two sentences to describe what this is and why it must be addressed?

Yes, we have added the sentence:

" The overlap factor corresponds to the overlap between the laser beam and the field of view of the telescope. It is equal to 1 when the two fields completely overlap and leads to a geometric attenuation of the lidar when the overlap is partial. It…"

45. Is the aircraft attitude (pitch, roll, yaw, etc.) data included any of the level 1, 1.5, etc data?

Yes, all data levels contain this information.

We have added the sentence:

" It should be noted that for Level 1 to Level-2, the location and attitude of the aircraft are also reported for each horizontal lidar profile."

in Section 5 (line 2 page 10).

46. Can the manuscript please state the size of the data files? For example, megabytes per file?

The sentence:

" The typical sizes of the different NetCDF files are: i) ~ 195-420 Mo for Level-1 data, ii) ~11-29 Mo for Level-1.5 data, iii) ~4-18 Mo for Level-2&3 cloud products, and iv) ~60-190 Ko for Level-2&3 aerosol products."

has been added at the end of subsection 6.2.

The authors would like to thank the reviewer for his/her valuable comments which helped improving the quality of the manuscript. Our point-by-point responses to the reviewer's comments appear in bold below.

Reviewer 2

General comments

The overall quality of the preprint is very good showing a well written manuscript. However, some technical corrections must be performed before publication.

Specific comments

No specific comments are raised when reviewing this manuscript.

Technical corrections
Page 1
L23. Replace "sensing" by "sensing techniques'
A correction has been done.
"…with the help of sidewards staring remote sensing instruments (lidar and radar)."

L25. Replace «made it » by « made »
The correction has been done.
"The measurements made possible to characterize the size distribution…"

Page 2
L14. Add more recent references (2019-2020)
The role of trade-cumuli in the uncertainty in model estimates climate sensitivity has been shown for the first time in 2005, but many papers have confirmed this result subsequently (Brient et al., 2016; Vial et al., 2017). More recent studies show that the uncertainty in model estimates of climate sensitivity still arises from the response of low-level clouds to warming (e.g. Zelinka et al., 2020), not only in the tropics but also in the extratropics, but no study to date has analyzed the relative roles of shallow cumuli vs stratocumuli in the uncertainty of low-cloud feedbacks. It is also worth noting that the models that predict a significant decrease of shallow cumuli with warming predict a higher climate sensitivity than the models that predict weak or no change.

"In climate models, the differing responses of these clouds to global warming has been identified as one of the leading causes of uncertainty in climate sensitivity (Bony and Dufresne, 2005; Medeiros et al., 2015; Webb et al., 2006)…"

has been replaced by:

"In climate models, the differing responses of these clouds to global warming has been identified as one of the leading causes of uncertainty in climate sensitivity (Bony and Dufresne, 2005; Brient et al., 2016; Medeiros et al., 2015; Vial et al., 2017)."

Added references are:

Brient, F., T. Schneider, Z. Tan, S. Bony, X. Qu and A. Hall, 2016: Shallowness of tropical low clouds as a predictor of climate models' response to warming. Clim. Dyn., 47 (1-2), 433-449, doi:10.1007/s00382-015-2846-0

Vial, J., S. Bony, B. Stevens and R. Vogel, 2017: Mechanisms and model diversity of trade-wind shallow cumulus cloud feedbacks: A review. Surveys of Geophysics, 38 (6), 1331-1353, doi:10.1007/s10712-017-9418-2

Page 3
L1. Replace « much better » by « very efficiently »
The correction has been done.
"In contrast, lidars have the potential to detect them very efficiently…"

L11. Omit « Both »
The correction has been done.
"To increase the areal sampling of the cloud field and to observe the cloud distribution at cloud-base…"

Page 4
L8. Define « LSCE »
It has been defined.
"Developed at LSCE (Laboratoire des Sciences du Climat et de l'Environnement)…"

Page 5
L12. Replace « (and » by « and »
The correction has been done.
" …pressure difference and a wave front error…"

L13. Replace « Flatness « by « The window Flatness »
The correction has been done.
"The window flatness was specified…"

Page 6
L23. The « prototypical flight » could be « flight strategy
The correction has been done.
" The flight strategy …"

Page 8
L8. Replace « boundary layer « by « Planetary boundary layer »
The correction has been done.
"…the lower part of the planetary boundary layer."

Page 10
L6. Replace « begining » with « starting »
The correction has been done.
"Figure 4. Lidar data processing diagram starting from raw data…"

L13. Replace "native" by "raw"
The correction has been done.
"The raw sampling…"

L15. Omit “it”
The correction has been done.
"This offset makes possible…"

Page 17
L5. Replace “nadir” by “nadir”
The correction has been done.
"…considered for lidar measurements at Nadir…"
has been replaced by:
"…considered for lidar measurements at nadir…"

Page 18
L1. Replace “consid, Fered » by “considered »
The correction has been done.
"Two additional parameters are considered for…"

Page 29
L5. Replace « further » by « forthcoming »
The correction has been done.
"… as the forthcoming Earth Clouds…"

Figures 3, 5, 6, 12:
Provide these figures with much higher resolution.

The figures will be in 300 dpi.

The authors would like to thank the reviewer for his/her valuable comments which helped improving the quality of the manuscript. Our point-by-point responses to the reviewer's comments appear in bold below.

Reviewer 3

General Comments:
This paper describes the different levels of data products from an airborne horizontal pointing aerosol lidar collected during the EUREC4A field campaign. The paper is well written and the data products are well described. However, the preprocessing of the data (Level 1→ Level 1.5) could be concise and some of the figures and tables could be removed without loss of information.

We note this Reviewer's concern, but also Reviewer #1's comment which goes in the opposite direction. As a compromise, we chose not to modify the level of details of the manuscript.

I was not able to access the data from the data archive. The doi s listed in the paper are correct and points to the archive but the data links within the doi pages are invalid or missing.

Yes, there was a problem on the site. It is now fixed. The access is now fine:

https://doi.org/10.25326/58

https://doi.org/10.25326/57

https://doi.org/10.25326/59

Specific Comments:

How were cloud base heights determined for the Phase 2 flight legs?

We have added the sentence:

"It should be noted that prior to the beginning of Phase 2, a best-guess estimate of the CBH, assessed from multiple sources of information (radiosoundings launched from BCO and research vessels, dropsondes released from other aircraft), was provided to the ATR-42 scientists via the onboard chat capability. The flight altitude was then adjusted using real-time lidar echoes, cloud droplets counts from cloud microphysics probes and visual observations by the pilots and the lidar operator through lateral windows."

at the end of Section 4.

What is the typical aircraft speed? I think this information would be useful for future readers.

Agreed, the typical aircraft speed is ~100 ms^{-1}.

We have added this information in Section 4:
"Note that during straight-line flights, the typical speed of the aircraft was ~100 ms^{-1}."

How do you separate the clouds along the flight direction? There is no information about clouds along the flight direction? I think you should be able to calculated cloud size distribution along the flight direction as well. Any reason for not including that as part of the L3 product?

We have added in Section 5.3.1.b the following sentence:

" It is worth noting that owing to the integration/acquisition time of the lidar measurement (5 s) and the aircraft speed (100 ms^{-1}), we are unable to derive a cloud mask along the direction of aircraft motion (the minimum distance we can resolve along this direction is 500 m, which is roughly the upper bound of the cloud chords measured along the line of sight of the lidar). The cloud mask distributed in the Level-2/Level-3 datasets thus corresponds to the cloud detection done along the line of sight of the lidar only."

Cloud cover from 0-4 km range would be another L3 product of interest.

We agree that the distribution of a cloud fraction product would be interesting. However, we feel that the users should better compute this diagnostic (as well as many others) themselves, as it is quite straightforward to compute based on the other distributed products and would make it possible for the users to tailor the diagnostics to their own needs.

What is the time resolution of the lidar profiles? P9, Line 7 would be a good place for this information.

Agreed. The time resolution is ~5s. This information was missing in the text and has been added in Section 5 (p9 line 7):

"The raw sampling of the lidar profiles is 0.75 m along the line of sight and an average over 50 shots is performed during the acquisition, corresponding to about one recording every 5 s (2.5 s averaging time and 2.5 s recording time)."

There is also no information about the horizontal resolution of the profiles. From figure 10, it looks like horizontal resolution is around 20-30 m?

Agreed. A sentence is missing in subsection 5.2.1 to provide the information. Such a sentence has now been added:

"To build level 1.5 data, the raw sampling along the line of sight has been degraded in order to ensure the independence of each point on the horizontal lidar profile. The final resolution is then 15 m. The ALiAS-derived level 1.5 data are then profiles corrected…"

Apparent Backscatter Coefficient (ABC): Why not call it attenuated backscatter coefficient? Or add a statement about how ABC is different from attenuated backscatter coefficient from other lidar (e.g. CALIOP).

The product can be called "Apparent Backscatter Coefficient" or "Attenuated Backscatter Coefficient", indifferently. In our case, we correct for molecular transmission and we preferred the term "apparent" as already used in previous papers. What is more important is how we define the variable ABC in equation (3). Nevertheless, we added to the text: "...Apparent Backscatter Coefficient (also referred to as Attenuated Backscatter Coefficient)".

Please include the range of viewing angle in a typical flight leg and what is the implication of this viewing geometry on the retrieved cloud size?

The effect of roll is taken into account in the quality indicator/flag (subsection 5.3.1.c, Table 4). It is less than 1±0.5° during Phase 2, and tough only very marginally impact cloud size

retrievals. As stated in the text, lidar profiles acquired during ATR-42 turns are discarded all together.

Are the viewing angle, aircraft attitude parameters included in the raw data? It would be also good to include an equation used to calculate the viewing angle in the text.

The field of view of the lidar is ~3 mrad irrespective of the attitude of the aircraft. Nevertheless, the roll can indeed influence the altitude of the area sampled by the lidar at a given distance from the aircraft. That is why there is a quality indicator included in the Level-2 data to flag lidar profiles acquired at non-negligible roll angles. The data also contains the angle between the horizontal and the direction of sight.

Please include values for T0 and T1 since it is mentioned in the text.

We have modified the sentence as:
" They take into account the transmissions of the parallel polarization of the two Brewster plates used: $T_0^{\parallel}$ for channel 0 ($T_0^{\parallel} \approx 0.45$) and $T_1^{\parallel}$ for channel 1 ($T_1^{\parallel} \approx 0.40$)."

It is not clear how the threshold for cloud detection is defined. What is coefficient Ce? How is Ce used for cloud detection? Could you use a single cloud detection threshold?

The cloud detection is performed in 2 steps:

1) Determination of cloud-free profiles during Phase 2 of a flight, to define a baseline clear sky profile and evaluate the noise level (standard deviation of the signal) as a function of the distance from the aircraft.
2) Comparison of each lidar profile to the baseline profile, taking into account the clear sky noise: a point is considered as cloudy if the ABC in this point exceeds Ce times the noise level. It is constant irrespective of the distance to the aircraft.

For the sake of clarity, we have replaced:

"For each lidar profile, it uses a threshold approach as already considered for lidar measurements at Nadir (Chazette et al., 2001; Shang and Chazette, 2014). The threshold is relative to the level of spread on the lidar signals in the absence of clouds. As for the aerosol products, a lidar profile is considered as being cloud-free if the logarithm of the ABC can be considered as linear with a relative error of less than 10% (cf. Section 5.3.2). The threshold is estimated for flight segments performed at a constant altitude (around the cloud base height, where molecular and particle scattering can be considered constant) and when the angle of the lidar line of sight with the horizontal does not exceed 3°. Lidar profiles acquired during ATR-42 turns are therefore excluded from the cloud level 2 data. The threshold varies with the distance from the aircraft. It is proportional (through a coefficient Ce) to the standard deviation of the cloud-free ABC signal determined for the rectangle under consideration."

by

" For each lidar ABC profile, it uses a threshold approach as already considered for lidar measurements at nadir (Chazette et al., 2001; Shang and Chazette, 2014). The threshold is proportional to the standard deviation of the noise of the cloud-free signal during Phase 2 of a given flight. Although the coefficient of proportionality Ce is constant, the threshold varies with the distance from the aircraft owing to the decrease of the signal to noise ratio (due to the increase of the clear-sky noise) away from the aircraft. As for the aerosol products, a lidar

profile is considered as being cloud-free if the logarithm of the ABC can be considered as linear with a relative error of less than 10% (cf. Section 5.3.2). The threshold is then calculated at a constant altitude (around the cloud base height, where molecular and particle scattering can be considered constant) and when the angle of the lidar line of sight with the horizontal does not exceed 3°. Note that the mean value is 1° and the standard deviation is 0.5°. Lidar profiles acquired during ATR-42 turns are therefore excluded from the cloud Level-2 data."

How do you define level of soiling? Is it like the entire flight is soiled or not?

The level of soiling is defined based on a strong attenuation through the aircraft window. This leads to a clear peak at range zero due to scattering, and a limitation of the lidar maximum range to around 4 km from the aircraft. In addition the soiling flag also takes into account the observations made by the operators during the flights and the state of the window after each flight.

How is the uncertainty in AEC for angular deviation calculated?

We have written " It should be noted that an angular deviation of 15° induces an error of 0.01 km^{-1} on the AEC." However, the angle of deviation is smaller than 1°.

Is Level 3 data calculated for each flight segment of a flight or entire flight? P24 Line 1 says entire flight but P9 Line 8 says flight segment?

Level-3 cloud products are calculated for data acquired during Phase 2, as for Level-2. For the aerosol products, it is calculated on all cloud-free profiles during the flight.

For the cloud products we have modified the first sentence as:

"Level-3 cloud products consist of probability distribution functions (PDFs) of cloud chords along the laser line of slight computed during Phase 2 of the flight."

Table 2: I don't think Table 2 is very useful in its current form. Potential data users are very likely not going to be looking for certain flight blocks. They might be more interested in a particular day. Information from Table 2 could be combined with Table 5.

Table 2 gives an overview of all the flights performed with the main flight blocks, while Table 5 presents the main characteristics of these flights. These two tables could be grouped together, but the result would be too imposing. Therefore, we have chosen to make two different tables which intervene at different places in the text.

Technical corrections:

P1, Line 22: add “instruments”
Agreed.

P6, Line 8: Change “Prototypical” to “Typical” ,
We use "Flight strategy"

P6, Line 13: Change “independently” to ‘independent”
Agreed.

P6, Line 17: Change (~9h00) to (~9h)
Agreed.

P6, Line 23: Change “A prototypical” to “An example”. Same for P9, Line 2.
We use "The flight strategy"

P6, Line 24: Change “needs” to “questions”,
We use " scientific requirements"

P8, Line 8 and 9: Complete the sentences between two bullet points
Agreed.
"…the planetary boundary layer.

5. The ATR-42 cruised…"

P9, Line 8: “For level 3 profiles are averaged over flight segments…” might be clearer if that is what it meant to be.
Agreed.
We have modified as:
"The statistics performed on Level-2 data are gathered in the Level-3 data. Statistics are computed for all flights for the aerosol Level-3 products and for the Phase 2 of the flights for the cloud products."

P11, Line 3: subscript of c for clouds would be more intuitive than n.
Agreed.

P12, Line 3: change “clouds” to “data points”
Agreed.

Equation 4 and 5: use parallel and perpendicular symbol for T0 and T1 respectively to be consistent.
Agreed.

P18, Line 1: typo “considered”
Agreed.

Table 4: B1 values for clear and clogged wind should be 0/1.
No, it is the detection or not of a cloud (0 or 1).

P23, Line 2: Separate into two sentences for clarity.

"The Barbados area is a region where a very wide variety of aerosols can be found, the main ones being marine aerosols to which can be added terrigenous aerosols and even biomass burning aerosols."

Has been replaced by

The Barbados area is a region where a very wide variety of aerosols can be found. The main ones are marine aerosols to which can be added terrigenous aerosols and even biomass burning aerosols.

P26, Line 11: Change to “test flight”

Agreed.

Trade-wind clouds and aerosols characterized by airborne horizontal lidar measurements during the EUREC^{4}A field campaign

Patrick Chazette[1], Julien Totems[1], Alexandre Baron[1], Cyrille Flamant[2], Sandrine Bony[3]

[1] LSCE/IPSL, CNRS-CEA-UVSQ, University Paris-Saclay, CEA Saclay, 91191 Gif sur Yvette, France

[2]LATMOS/IPSL, CNRS-UPMC-UVSQ, Sorbonne Université, Campus Pierre et Marie Curie, 75252 Paris, France

[3]LMD/IPSL, CNRS, Sorbonne Université, Campus Pierre et Marie Curie, UPMC, 4 Place Jussieu, 75252 Paris, France

Correspondence to: Patrick Chazette (patrick.chazette@lsce.ipsl.fr)

Abstract. From 23 January to 13 February 2020, twenty manned research flights were conducted over the tropical Atlantic, off the coast of Barbados (-58°30' W 13°30'N), to characterize the trade-wind clouds generated by shallow convection. These flights were conducted as part of the international EUREC^{4}A (Elucidating the role of clouds-circulation coupling in climate) field campaign. One of the objectives of these flights was to characterize the trade-wind cumuli at their base for a range of meteorological conditions, convective mesoscale organizations and times of the day, with the help of sidewards staring remote sensing instruments (lidar and radar). This paper presents the datasets associated with horizontal lidar measurements. The lidar sampled clouds from a lateral window of the aircraft over a range of about 8 km, with a horizontal resolution of 15 m, over a rectangle pattern of 20 km by 130 km. The measurements made possible to characterize the size distribution of clouds near their base, and the presence of dust-like aerosols within and above the marine boundary layer. This paper presents the measurements and the different levels of data processing, ranging from the raw Level-1 data (https://doi.org/10.25326/57; Chazette et al., 2020c) to the Level-2 and Level-3 processed data that include an horizontal cloud mask (https://doi.org/10.25326/58; Chazette et al., 2020b) and aerosol extinction coefficients (https://doi.org/10.25326/59; Chazette et al., 2020a). An intermediate level, companion to Level-1 data (Level-1.5), is also available for calibrated and geolocalized data (https://doi.org/10.25326/57; Chazette et al., 2020c).

Keywords: EUREC^{4}A, cloud mask, shallow cumulus, cloud base height, aerosol extinction, dust, Tropical West Atlantic Ocean, Barbados

1 Introduction

Subtropical regions play a major role in the radiation balance of the Earth due to their dry free troposphere and their ability to emit a large amount of heat to space (Pierrehumbert, 1995). Within the marine boundary layer, these regions are associated with low-level clouds that also contribute to cool the Earth through the reflection of sunlight. In the trade-wind regimes, the prevailing clouds are shallow cumuli (Norris, 1998). They are so ubiquitous that their response to changes in the environment has the potential to greatly influence the global radiation budget. In climate models, the differing responses of these clouds to global warming has been identified as one of the leading causes of uncertainty in climate sensitivity (Bony and Dufresne, 2005; Brient et al., 2016; Medeiros et al., 2015; Vial et al., 2017). The models that predict a significant decrease of shallow cumuli with warming predict a higher climate sensitivity than the models that predict weak or no change. To assess the credibility of climate projections, it is thus necessary to understand how these clouds interact with their environment.

This was one of the main motivations of the EUREC^{4}A (*Elucidating the role of clouds-circulation coupling in climate*) field campaign which took place in January-February 2020 over the western tropical Atlantic, West of Barbados (Stevens et al., in prep). This experiment was originally designed to test our understanding of low-cloud feedbacks (Bony et al., 2017), especially the physical processes that control the cloud fraction around cloud base, where climate models predict the largest changes in cloudiness with warming. In addition, clouds in the trade-wind regimes exhibit prominent forms of convective organization (Stevens et al. 2020), and the mesoscale cloud patterns depend on environmental conditions and influence the reflection of sunlight (Bony et al., 2020). The question thus arises as to whether changes in the mesoscale organization of clouds might play a role in low-cloud feedbacks (Nuijens and Siebesma, 2019). Answering this question constitutes another key objective of the EUREC^{4}A campaign. To address these issues, EUREC^{4}A aimed at characterizing the field of trade cumuli, in particular the horizontal cloud coverage around cloud base, the spatial arrangement and the size distribution of clouds, through complementary platforms and instruments, including airborne lidars.

Indeed, from a remote sensing point of view, shallow cumuli count among the most challenging clouds. They are small, broken, and sometimes very optically thin, so their detection from

radiometry can be difficult. In contrast, lidars have the potential to detect them much better (Liou and Schotland, 1971; Spinhirne et al., 1982). Space-borne lidars associated with missions such as LITE (Lidar In-space Technology Experiment, Winker 1996), GLASS (Geoscience Laser Altimeter System, Palm et al. (2005); Spinhirne et al. (2005)), CALIPSO (Cloud-Aerosol LIdar with Orthogonal Polarization, Winker et al. (2003)), or more recently CATS (Cloud-Aerosol Transport System, Yorks et al. (2016)), have even revolutionized our knowledge of the global distribution of clouds (Berthier et al., 2004). However, cloud observations from ground-based, airborne or satellite lidar technology were made at nadir or zenith. Due to the overlap of cloud layers, this can make the observation of the cloud fraction around cloud base difficult. Moreover, the laser beam is so thin that it can only sample a tiny fractional area of the cloud field, especially in regions where the cloud fraction rarely exceeds 10%. To increase the areal sampling of the cloud field and observe the cloud distribution at cloud-base, EUREC^{4}A introduced a new sampling approach, consisting in using an aircraft carrying a sidewards-staring lidar. This strategy was realized by implementing the Airborne Lidar for Atmospheric Studies (ALiAS) (Chazette et al., 2012b) with an horizontal line-of-sight in the ATR-42 of SAFIRE (the Service des Avions Français Instrumentés pour la Recherche en Environnment), using a modified lateral window on the aircraft. An horizontally-looking cloud radar was also implemented on the same aircraft to complement the lidar observations and benefit from the lidar-radar synergy for the detection of clouds.

Horizontal lidar measurements do not only have a great potential for the observation of clouds, but also for the characterization of aerosols. During the AMMA (African Monsoon Multidisciplinary Analysis, Redelsperger et al. (2006)) campaign, Chazette et al. (2007) mounted a lidar on an ultralight aircraft and showed that if the atmosphere is horizontally homogeneous along the line of sight, horizontal shooting directly gives access to the extinction coefficient of aerosols without any hypothesis on their nature (Chazette et al., 2007). The same approach was used during the Dust and Biomass burning aerosol Experiment (DABEX) with a combination between lidar measurements from an ultra-light aircraft and in situ measurements from the UK FAAM aircraft (Johnson et al., 2008). Therefore, during EUREC^{4}A the horizontal lidar measurements made from the ATR-42 were also used to characterize the marine boundary layer and long-range transports of aerosols within the free troposphere.

The goal of this paper is to present the flight strategy, measurements, data processing and cloud and aerosol products derived from the horizontal lidar measurements made during the EUREC^{4}A campaign. Section 2 presents the ALiAS lidar characteristics and Section 3 the

implementation of the lidar in the ATR-42 aircraft. The flight plan and its decomposition into different phases are presented in Section 4. Section 5 describes the different levels of data processing and the cloud and aerosol products that constitute the final dataset. The conclusion is presented in section 6 as well as how to access the data.

2 Lidar characteristics

The ALiAS lidar was flown onboard the ATR-42 (Figure 1) of SAFIRE off the east coast of Barbados. Developed at LSCE (Laboratoire des Sciences du Climat et de l'Environnement) following a precursor instrument (Chazette et al., 2007), ALiAS is based on a frequency-tripled Nd:YAG laser (ULTRA-100) manufactured by Lumibird/QUANTEL emitting at the wavelength of 355 nm. It satisfies eye safety requirements (EN60825-1) at the output window considering the characteristics given in Table 1 (emitted wavelength, pulse energy, repetition rate, beam diameter and pulse duration). The UV pulse energy is 30 mJ and the pulse repetition rate is 20 Hz. The acquisition system is based on a PXI-5124 (PCI eXtensions for Instrumentation) fast digitizer working at 200 MHz and 12 bits, without going through a pulse (photon) counter leading to an initial resolution along the line of sight equal to 0.75 m. Using co- and cross-polarized channels relative to the linear polarization of the emitted radiation, ALiAS was designed to monitor the cloud, aerosol and hydrometeor distributions and dispersions in the low and middle troposphere from aircrafts. It was successfully used on board the Falcon 20 of SAFIRE to monitor and study the ash plume following the eruption of the Eyjafjallajökull volcano eruption (Chazette et al., 2012b). The main characteristics of ALiAS are given in Table 1.

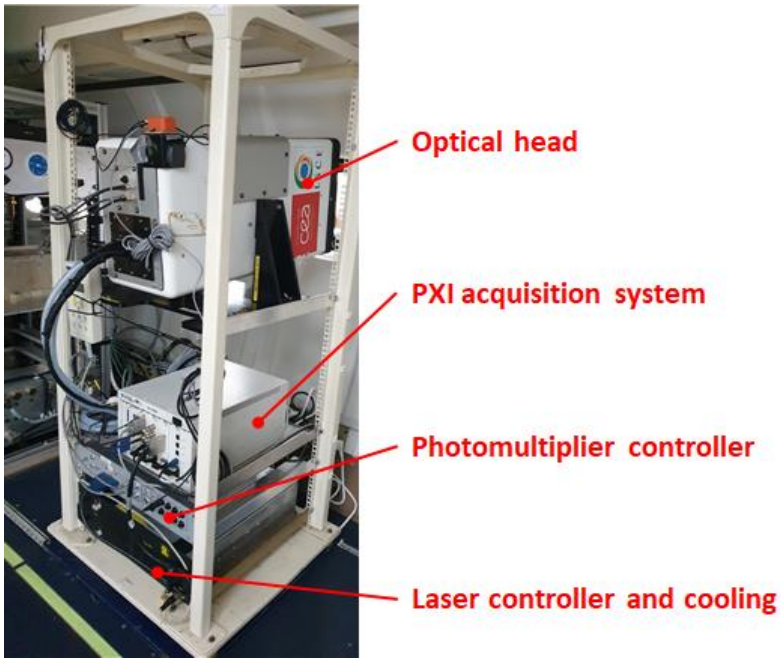

Figure 1. ALiAS on board ATR-42 during the EUREC^{4}A campaign.

Table 1. Characteristics of ALiAS on board the ATR-42 during the EUREC^{4}A airborne campaign.

Wavelength	355 nm
Pulse repetition rate	20 Hz
Pulse duration	8 ns
Beam diameter	25 mm
Divergence	<0.2 mrad
Reception diameter	150 mm
Filter bandwidth	0.2 nm
Field of view	3 mrad
Detector	Photomultiplier
Detection mode	Analogue
Digitalization	12 bits
Native line of sight resolution	0.75 m
Dimensions of the optical head	45 cm (height) 28 cm (width) 18 cm (deep)
Weight of the optical head	~15 kg
Weight of the electronics	~20 kg
Power supply	220 V AC
Consumption	<500 W

3 Implementation in the aircraft

ALiAS was installed in the aft of the ATR-42 aircraft in an orientation that enabled a direct near-horizontal line-of-sight. Its orientation was measured at all time by an inclinometer. The only possible solution for such an implementation, in compliance with aviation regulation, i.e. without complex modifications to the structure or aerodynamics of the aircraft, was to adapt an optical window with a custom frame inside an existing passenger window (Figure 2). UV fused silica was chosen to ensure correct transmission of several useful lidar wavelengths (355, 532, 830, 1550, 2000 nm) at affordable cost. The frame being 244 mm x164 mm, a 20 mm thickness was sufficient to ensure both a safety factor of ~6 for mechanical resistance to air pressure difference and a wave front error below λ/20 at 355 nm (Spark and Cottis, 1973). The window flatness was specified to λ/4 at 633 nm, with an optical coating of 315 nm of MgF2 to reduce theoretical reflection losses to around 4%. The ~15° inclination of the window due to the curvature of the plane fuselage avoids harmful effects of the reflected beam inside the lidar, as long as the receiving aperture is above the emitting aperture, but extra beam tubing was found to be necessary to limit the impact of diffuse echoes on the sensitive lidar detectors.

A specific study and certification were performed by SAFIRE itself to install the window at the back of the ATR-42 aircraft, on the starboard side. The optical head of ALiAS was already in a fiberglass container adapted to aircraft operation. As shown in Figure 1, a standard aircraft-certified 19-inch rack structure was fitted with a carrying structure for this container, and the elements of the lidar electronics installed below, making the lidar system an easily mounted and self-contained unit. It was operated in-flight from a passenger sitting in front of an in-flight checkpoint, allowing real time validation of the cloud base altitude sampling.

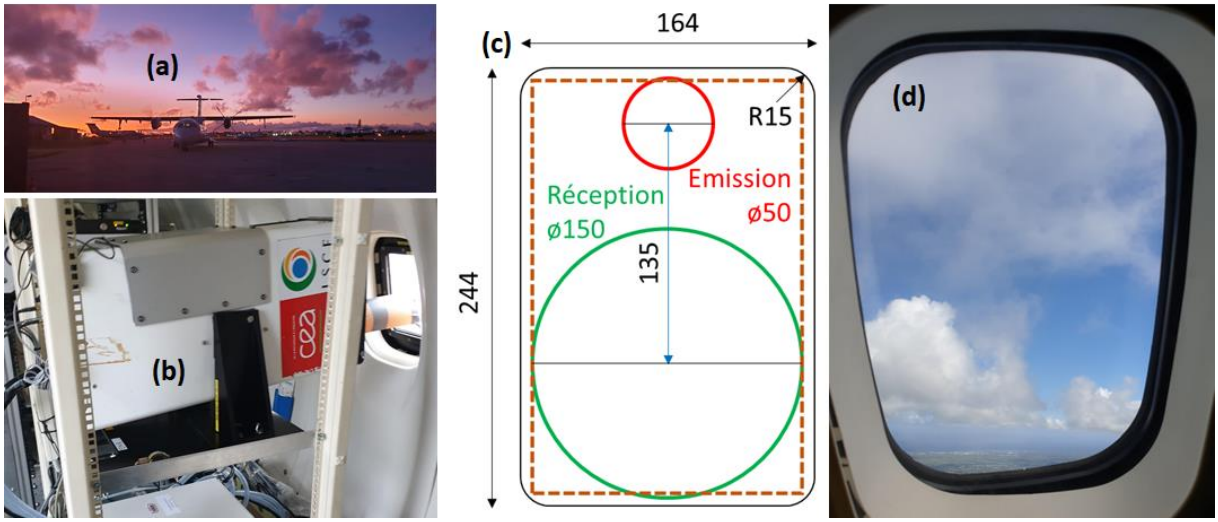

Figure 2. Location of the ALiAS lidar in the ATR-42 (a). The lidar is placed horizontally (b) and the laser beam is guided to the MgF2 window (c) to avoid laser reflections. Window (c) has replaced a passenger window (d) in the back of the aircraft.

4 Flight strategy

The flight strategy was defined well before the intensive campaign and presented in Bony et al. (2017). It has been adapted to take into account the ATR-42 autonomy and the coordination with the other platforms involved in EUREC^{4}A. The goal being to achieve a statistical sampling of the cloud fields, each flight repeated more or less the same flight plan, twice a day, independent of weather conditions.

On a given day of operation, the ATR-42 generally performed two flights, each flight having a duration of ~4h. The take-off time of the ATR-42 was tightly coordinated with that of the High Altitude and Long-Range Research Aircraft (HALO) operated by of DLR (Deutsches Zentrum für Luft- und Raumfahrt). The endurance of the HALO (~9h) allowed the 2 ATR-42 flights to be conducted within the timeframe of a single HALO flight, taking into account the time for refuelling at Grantley Adams International Airport (GAIA) in between ATR-42 flights. Most of the ATR-42 flying time was spent off the east coast of Barbados within the so-called HALO

circle, along which HALO released dropsondes and observed the atmosphere at nadir with a radar, a lidar and multiple radiometers (Stevens et al., 2019).

The flight strategy is illustrated in Figure 3 for the flight on 26 January 2020. It was built along 5 major phases (see Table 2), which contributed to the multi-aircraft and statistical sampling strategy implemented during the field campaign. Note that during straight-line flights, the typical speed of the aircraft was ~100 ms^{-1}. Each phase was designed to address particular scientific requirements of the lidar and other remote sensing and in situ instruments composing the ATR-42 payload (radar, aerosol and cloud microphysics, water vapour stable isotopes using cavity ring-down spectrometry, turbulence):

1. On the way to the HALO circle, the ferry time was dedicated to perform an aircraft sounding up to 2.5-4.5 km above mean sea level (a.m.s.l.) to describe the vertical thermodynamical and dynamical structure of the lower atmosphere and obtain a first guess of the location of cloud and aerosol layers. Such an aircraft sounding was aimed at retrieving aerosol extinction coefficient and volume depolarization ratio profiles from the lidar measurements (see subsection 5.3.2) and assess whether the upper part of the sounding was conducted in aerosol-free and/or cloud-free conditions. It is worth noting that several episodes of dust transport from West Africa were evident from the lidar data during the campaign.

2. Upon arriving in the HALO circle, the ATR-42 started performing two or three north-south oriented rectangles (roughly orthogonal to the trade winds), approximately 130 km long and 20 km wide. Each rectangle was flown in 45-50 min. The northwestern and southwesternmost corners of the rectangle were positioned 10 Nm (1 Nm = 1.852 km) to the west of the HALO circle. In the event that the ATR-42 circuit only included two rectangles, they were *always* performed around the cloud base height (CBH). When the circuit included three rectangles, on some occasions, the ATR-42 performed the 1st rectangle near the altitude of the ferry, mainly to sample stratiform clouds near the inversion level or the air just above. In such cases, the sideways-pointing lidar ALIAS allowed the characterisation of the variability of aerosol-related extinction within the HALO circle in cloud-free conditions, or was used to obtain a cloud mask and further statistics on the properties of stratiform clouds, whenever they were present at the altitude of the flight. The second and third rectangles were always performed at CBH, to collect statistics on the spatial distribution of marine boundary layer clouds, measure the cloud base cloud fraction, and provide a cloud mask. Figure 3 shows an example of

flight plan during which the 3 rectangles were performed at CBH on 26 January. On one occasion (on February 9) the ATR-42 circuit comprised four rectangles performed at CBH (see Table 2),

3. After the rectangles, the ATR-42 performed two long L-shape legs (of 20-25 min each) below CBH, one near the top and the middle of the subcloud-layer. The first part of the L-shape leg consisted of a ~70 km long east-west oriented run (approximately parallel to the mean trade winds) and the second part of the L, also ~70 km long, was oriented perpendicularly to the first part. The return-trip along the L-shape legs was generally performed at the same altitude (see Figure 3). These legs were essentially designed to characterise the turbulent structure of the marine boundary layer. In our case, they also allowed characterizing the extinction and polarizing capability of aerosols present in the marine boundary layer,

4. At the end of the return trip along the second L-shape run, the ATR-42 generally performed an ultra-low pass at 60 m above sea level for ~10 min in order to measure turbulent heat fluxes and marine aerosols within the lower part of the planetary boundary layer.

5. The ATR-42 cruised back towards Barbados around 3 km a.m.s.l. (see Figure 3). Meanwhile, the aircraft soundings allowed a second retrieval of aerosol extinction coefficient and volume depolarization ratio profiles which were used to assess how the geometrical and optical properties of aerosol layers evolved in the course of the flight.

The flight strategy was sometimes slightly adjusted based on the meteorological situation, e.g. depending on the presence of a stratiform cloud layer near the trade inversion level. The details on the ATR-42 flight blocks (rectangles, L-shape legs, surface legs) are given in Table 2. It should be noted that prior to the beginning of Phase 2, a best-guess estimate of the CBH, assessed from multiple sources of information (radiosoundings launched from BCO and research vessels, dropsondes released from other aircraft), was provided to the ATR-42 scientists via the onboard chat capability. The flight altitude was then adjusted using real-time lidar echoes, cloud droplets counts from cloud microphysics probes and visual observations by the pilots and the lidar operator through lateral windows.

Table 2: Main flight blocks (rectangles, L-shape legs, surface legs) for the ATR42 flights as well as flights date.

Type of flight blocks	**ATR42 flight number (FXX) and date (DD.M)**
4 rectangles at CBH	F16 (09.2)

3 rectangles at CBH	F04 (26.1), F05 (28.1), F06 (30.1), F07 (31.1), F08 (31.1), F10 (02.2), F12 (05.2), F14 (07.2), F15 (09.2), F18 (11.2)
2 rectangles at CBH	F03 (26.1), F09 (02.2), F11 (05.2), F13 (07.2), F17 (11.2), F20 (13.2)
1 rectangle at stratiform cloud level	F11 (05.2), F13 (07.2), F17 (11.2), F19 (13.2)
2 L-shape legs below CBH	F03 (26.1), F04 (26.1), F05 (28.1), F06 (30.1), F07 (31.1), F08 (31.1), F19 (13.2), F10 (02.2), F11 (05.2), F12 (05.2), F14 (07.2), F15 (09.2), F17 (11.2), F18 (11.2), F19 (13.2)
Surface flux leg	F03 (26.1), F04 (26.1), F06 (30.1), F10 (02.2), F11 (05.2), F12 (05.2), F13 (07.2), F14 (07.2), F15 (09.2), F16 (09.2), F18 (11.2), F19 (13.2), F20 (13.2)

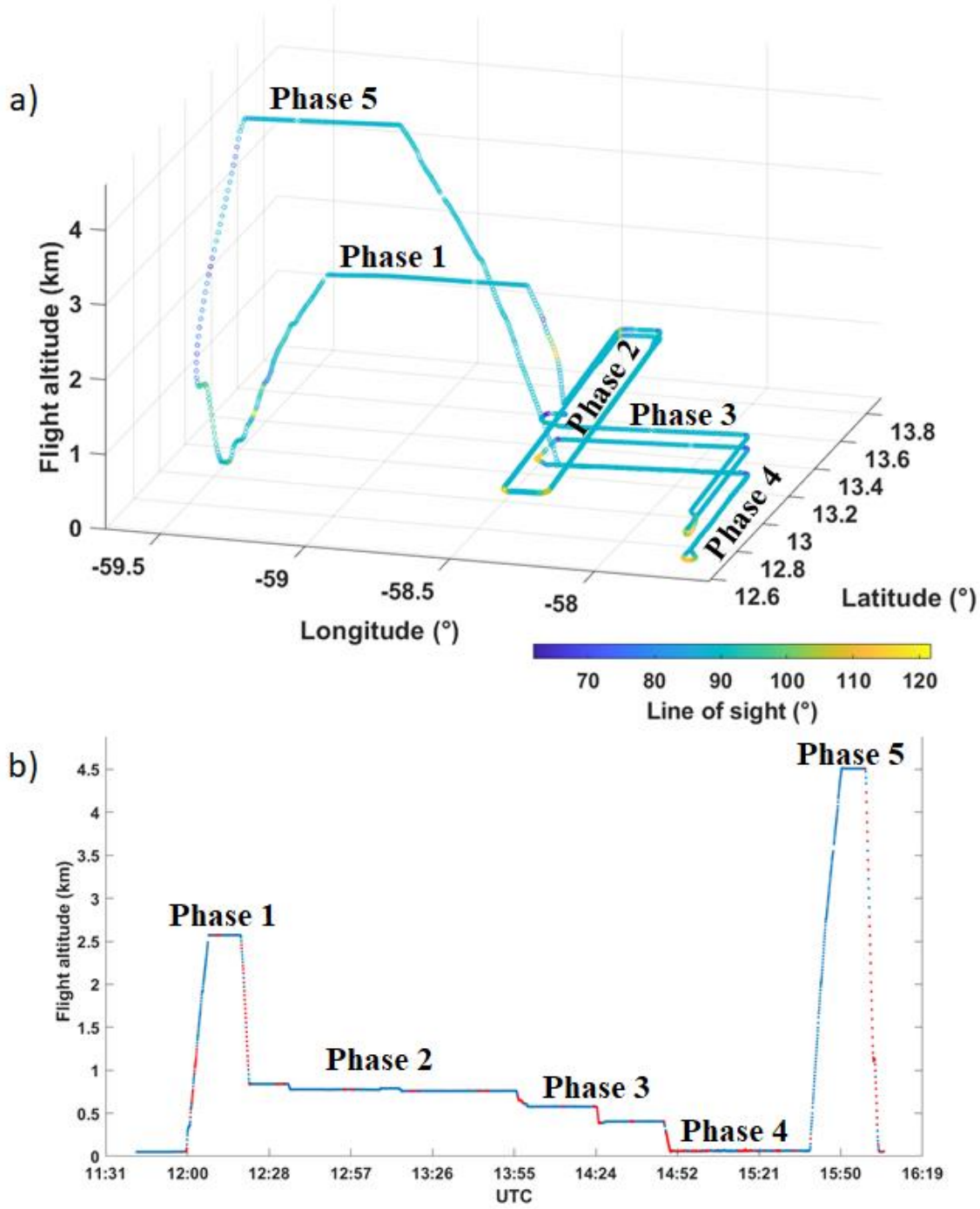

Figure 3. Flight strategy of ATR-42 loading ALiAS for flight #04 on 26 January 2020. The 5 phases of the flight are highlighted.

5 Data type

The data are presented from their raw form to the analytical products. They are classified into Level 1 to Level-3 as defined in Table 3. Up to Level-2 (included), lidar profiles are processed on an individual basis. The statistics performed on Level-2 data are gathered in the Level-3 data. Statistics are computed for all flights for the aerosol Level-3 products and for the Phase 2 of the flights for the cloud products. The step from Level-1 data to the final products of Level-2

and Level-3 is schematized in Figure 4. This section presents the steps taken to derive data products. The data recording format is detailed in Section 6. It should be noted that for Level-1 to Level-2, the location and attitude of the aircraft are also reported for each horizontal lidar profile.

Table 3. Data level with their type and main derived products.

Data level	Data type	Main products
1	Raw geolocalized data	Raw profiles recorded by the acquisition system
1.5	Range corrected lidar data	Background radiance (BR) Overlap function (F) Apparent Backscatter Coefficient (ABC) calibrated linear Volume Depolarization Ratio (VDR)
2	Inverted data	Cloud mask associated with each profile Aerosol Extinction Coefficient (AEC)
3	Statistical data	Probability density functions of cloud width (PDF) Mean vertical profile of AEC

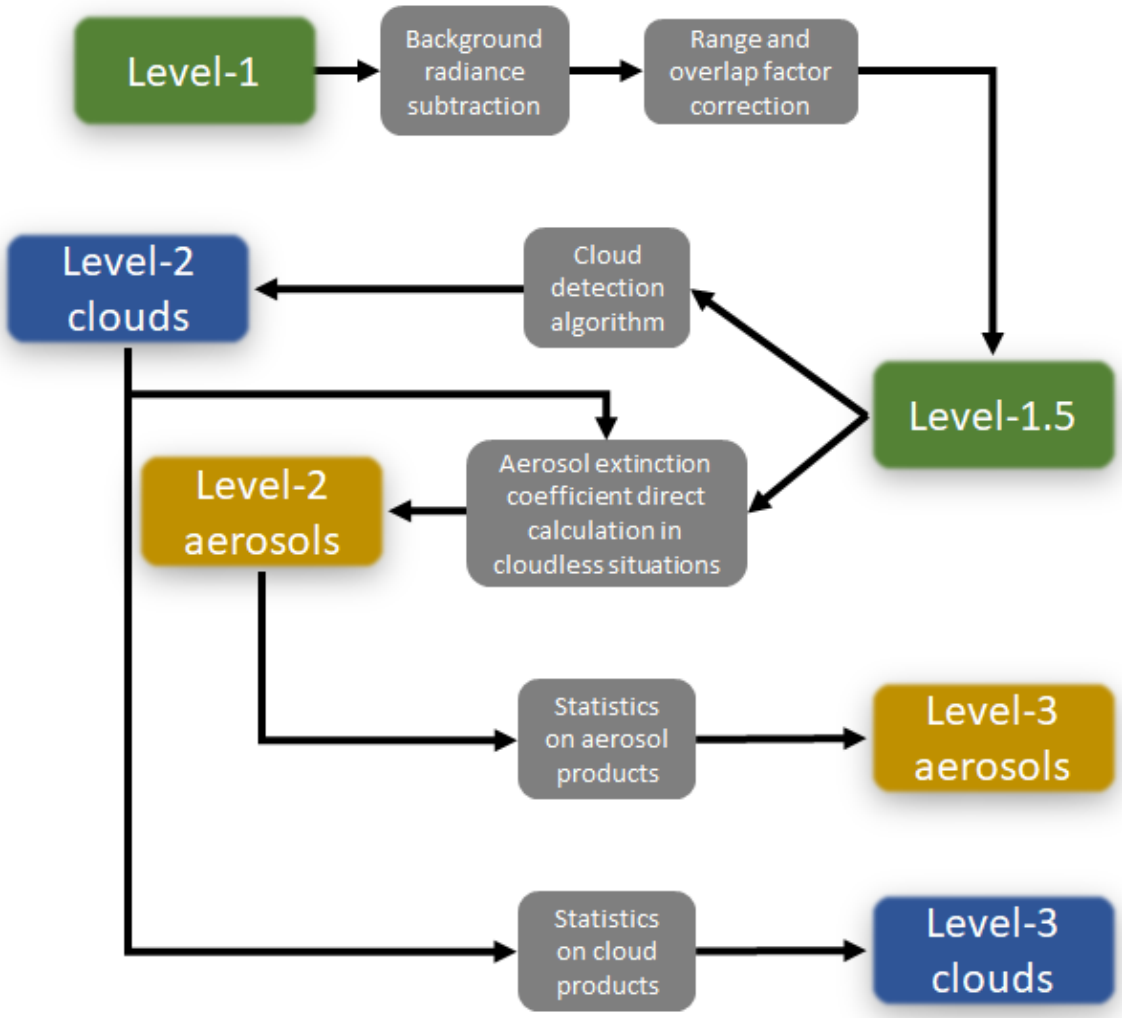

Figure 4. Lidar data processing diagram starting from raw data (1) and calibrated data (Level-1.5) to products (Level-2 and Level-3). The grey cells summarize the actions to be implemented for the data processing. The green color refers to data level in the pre-processing phase. Level-2 and Level-3 are subdivided in clouds (blue) or aerosols (orange) products.

5.1 Level-1

5.1.1 Description

Level-1 data are raw data expressed in volts. They are the result of time sampling at a frequency of 200 MHz. The raw sampling of the lidar profiles is 0.75 m along the line of sight and an average over 50 shots is performed during the acquisition, corresponding to about one recording every 5 s (2.5 s averaging time and 2.5 s recording time). The first 2000 points are recorded before the laser emission is triggered. This offset makes possible to record for each profile the contribution of the background sky radiance (BR) to the lidar signal (scattering of solar

radiation in the atmosphere). This contribution must then be corrected during the pre-processing process.

The lidar signal *S*, for each polarisation channel, of Level-1 data is expressed in the measurement configuration adopted for EUREC^{4}A as

$$S(x,z) = \frac{C}{x^2} \cdot F(x) \cdot \left(\beta_m(z)+\beta_a(z)+\beta_c(x,z)\right) \cdot \exp\left[-\frac{2}{\cos(\theta(z))} \cdot \left(\tau_m(\mathrm{x})+\tau_a(\mathrm{x})+\tau_c(\mathrm{x},z)\right)\right] + BR(z) \quad (1)$$

In this expression, the signal *S* depends on both the horizontal distance to the aircraft *x* and the flight altitude *z*. The system constant *C* is a function of various components of the lidar system such as the emitted energy and the quantum efficiency of the detectors *(e.g. Shang and Chazette, 2015)*. The overlap factor *F* characterizes the overlap between the transmission and receiving fields of view and must be determined to exploit near-field data. As the laser beam propagates through the atmosphere, it is backscattered by air molecules (subscript *m* in the following), aerosols (subscript *a*) and/or clouds (subscript *c*) towards the receiving system. This interaction is characterized by the volume backscattering coefficient β_k (k = *m*, *a* or *c*). The laser radiation is also attenuated by the atmospheric medium via the same actors and this attenuation is quantified by the optical thickness τ which is defined as a function of the extinction coefficient α_k by the relation

$$\tau_k(\mathrm{x},z) = \int_0^{\mathrm{x}} \alpha_k(x') \cdot dx' \quad (2)$$

Eq. (1) assumes that the optical properties of molecules and aerosols remain constant along the line of sight. A deviation from this assumption can be easily verified on Level-1.5 data, as will be shown. In the presence of clouds, the heterogeneity is too strong for this hypothesis to be true.

As the laser beam emitted from the aircraft may not be completely horizontal, a viewing angle θ (with respect to the true horizon) must be taken into account. In addition to Level-1 data, the aircraft attitude parameters (pitch, roll, heading) that allow to assess θ are recorded, as well as the geo-positioning of the measurements (longitude, latitude and altitude).

5.1.2 Baseline check

Baseline distortion can significantly increase the rates of non-detection and/or false detection of cloud structures. Hence, in Level-1 data, potential drifts of the lidar signal baseline are checked for each flight, in order not to introduce any bias during data processing, mainly in the

far field (i.e. beyond 4-5 km). This is done by comparing the BR from the pre-trigger with that computed in the far field, where the laser backscatter contribution becomes negligible, beyond 8 km in our case. As an example, Figure 5 shows the scatter plots of the BR computed on all the lidar profiles for the two channels of ALiAS on 26 January 2020. There is a little more spread on the parallel channel because it is more energetic than the perpendicular channel and the contribution of the laser can still exist beyond a horizontal distance of 8 km. Nevertheless, it is noticeable that for both channels the scatterplot data points are aligned along a straight line of slope 1, so there is no noticeable deviation from the baseline over the whole useful distance range (between 0 and 8 km).

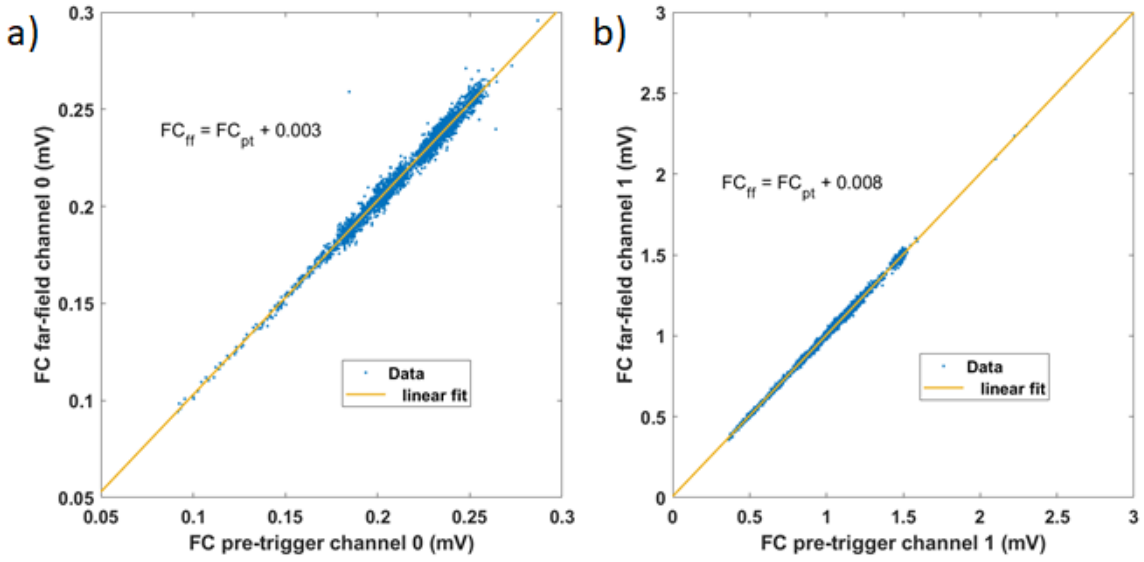

Figure 5. Verification of the linear behaviour of the relationship between the background sky radiance (FC) computed on the pre-trigger (FC_{pt}) and far-field (beyond 8 km in horizontal distance, FC_{ff}) for a) the parallel and b) the perpendicular channels. The example presented is from flight F03 on 26 January 2020.

5.2 Level-1.5

5.2.1 Description

To build Level-1.5 data, the raw sampling along the line of sight has been degraded in order to ensure the independence of each point on the horizontal lidar profile. The final resolution is then 15 m. The ALiAS-derived Level-1.5 data are then profiles corrected from both geometric factor and solid angle of detection. They are also corrected for molecular transmission via the molecular optical thickness τ_m to produce the Apparent Backscatter Coefficient (ABC, also referred to as Attenuated Backscatter Coefficient) which is expressed as

$$ABC(x,z) = (S(x,z) - BR(z)) \cdot \frac{x^2}{F(x)} \cdot \underbrace{\exp\left[\frac{2}{\cos(\theta(z))} \cdot \tau_m(\mathrm{x})\right]}_{\text{molecular transmission}} \quad (3)$$

An example of the ABC for the flight on 28 January 2020 is given in Figure 6. The ABC decreases away from the plane because of attenuation by aerosols and clouds (passing from orange to green on Figure 6a).In parallel with the ABC profiles, the volume depolarization ratio (VDR) is calculated from the two polarized lidar channels according to a procedure explained in (Chazette et al., 2012a, 2012b) . The relationships are recalled below. They take into account the transmissions of the parallel polarization of the two Brewster plates used: $T_0^{\parallel}$ for channel 0 ($T_0^{\parallel} \approx 0.45$) and $T_1^{\parallel}$ for channel 1 ($T_1^{\parallel} \approx 0.40$). The signals on the two lidar channels contain a contribution of the complementary polarization. The VDR is then expressed as a function of the ratio of the gains Rc of the two channels:

$$VDR(x,z) \approx \frac{T_1^{//} \cdot (S^{\perp}(x,z) - BR^{\perp})}{R_c \cdot (S^{\parallel}(x,z) - BR^{\parallel})} - \left(1 - T_0^{\parallel}\right) \cdot \left(1 - T_1^{\parallel}\right) \quad (4)$$

with

$$R_c \approx \frac{(S^{\perp}(x,z) - BR^{\perp}) \cdot T_1^{\parallel}}{(S^{\parallel}(x,z) - BR^{\parallel})\left[\left(1 - T_0^{\parallel}\right) \cdot \left(1 - T_1^{\parallel}\right) + VDR_m\right]} \quad (5)$$

The molecular volume depolarization ratio VDR_m is equal to 0.3945% at 355 nm (Collis and Russel, 1976). The term $\left(1 - T_0^{\parallel}\right) \cdot \left(1 - T_1^{\parallel}\right)$ measures how the lidar system is affected by imperfect separation of polarizations. The laser residual cross-polarization of 0.002 can be neglected for ALiAS. The calibration of the depolarization consists in estimating R_c from measurements in a molecular atmosphere, above any aerosol layer. The flight of January 25 around Barbados was dedicated to this calibration with an excursion of the aircraft above 4.5 km a.m.s.l. The calibration obtained is shown in Figure 7a. The variability of R_c is less than 2%, which leads to an absolute error on the VDR of the order of 0.2%. It is verified *a posteriori* that there is little aerosol at the calibration altitude, as shown (Figure 7b) by the vertical profile of the aerosol extinction coefficient for the flight considered (cf. Section 5.3).

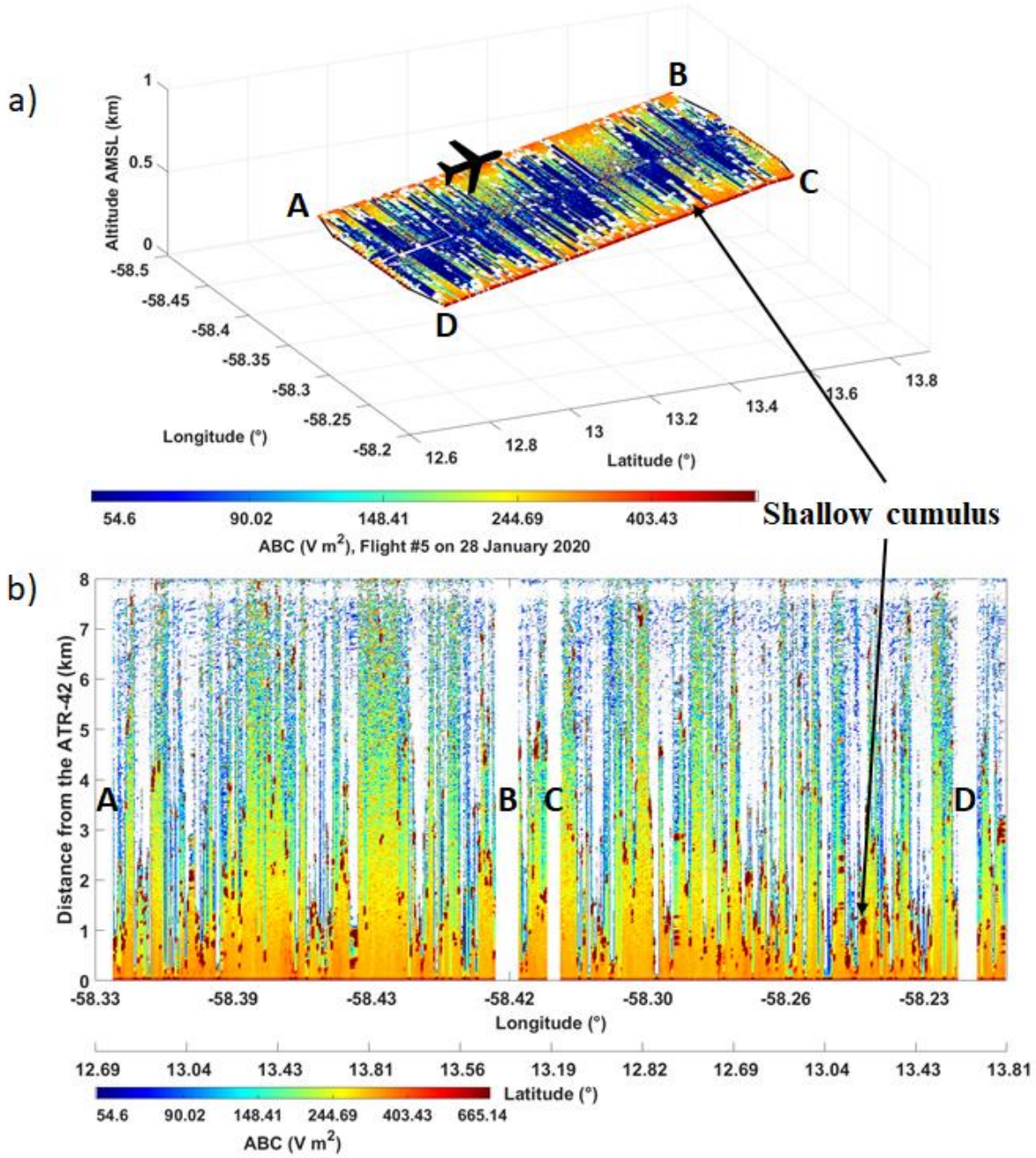

Figure 6. Example of the apparent backscatter coefficient (ABC) for the flight F05 on 28 January 2020, for the first rectangle of Phase 2. The lidar data in (a) is presented as a nearly horizontal map of ABC (with each data point being geo-localized in space as a function of latitude, longitude and altitude) which is used to identify the clouds within the rectangle ABCD described by the ATR-42 . (b) shows the same data as a function of longitude and distance from the aircraft. The clouds are color-coded in white in (a) and brown in (b).

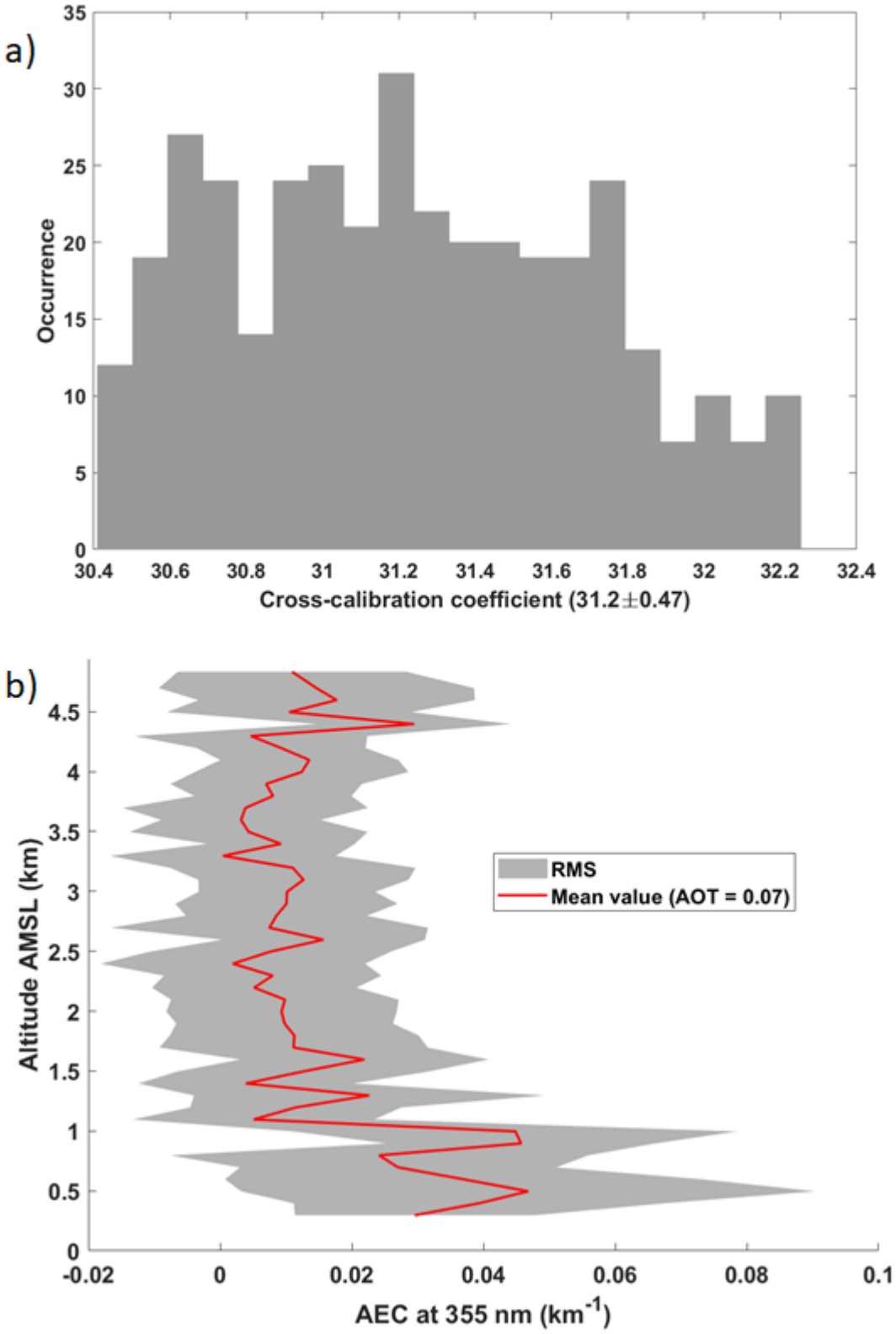

Figure 7. a) Calibration coefficient R_c of the volume depolarization ratio (VDR) derived from flight altitude above 4.5 km on 25 January 2020 (flight F04). b) Vertical profile of the average aerosol extinction coefficient (AEC) with its root mean square variability (RMS) for the flight

range on 25 January 2020. It corresponds to the Level-3 aerosol product. The aerosol optical thickness (AOT) is also reported.

5.2.2 Overlap factor

The overlap factor corresponds to the overlap between the laser beam and the field of view of the telescope. It is equal to 1 when the two fields completely overlap and leads to a geometric attenuation of the lidar when the overlap is partial. It can be computed from horizontal shots as previously performed for ALiAS during flights with an ultralight aircraft (Chazette et al., 2018). This calculation requires an homogeneous atmosphere along the line of sight of the lidar over a distance of about 1.5 km from the aircraft. To ensure this homogeneity, we performed the calibration at high altitude during the flight of 25 January 2020, above 4.5 km a.m.s.l., where the scattering is essentially molecular. The overlap factor of the two ALiAS channels is given in Figure 8. It is similar for both channels beyond 300 m distance from the emission. Compared to the theoretical overlap factor due to purely geometric effects, it shows a slight bump which is related to a non-zero angle of incidence on the interference filters of the lidar, for rays coming from the far field. This small deviation is nevertheless corrected for Level-2 and Level-3 processing.

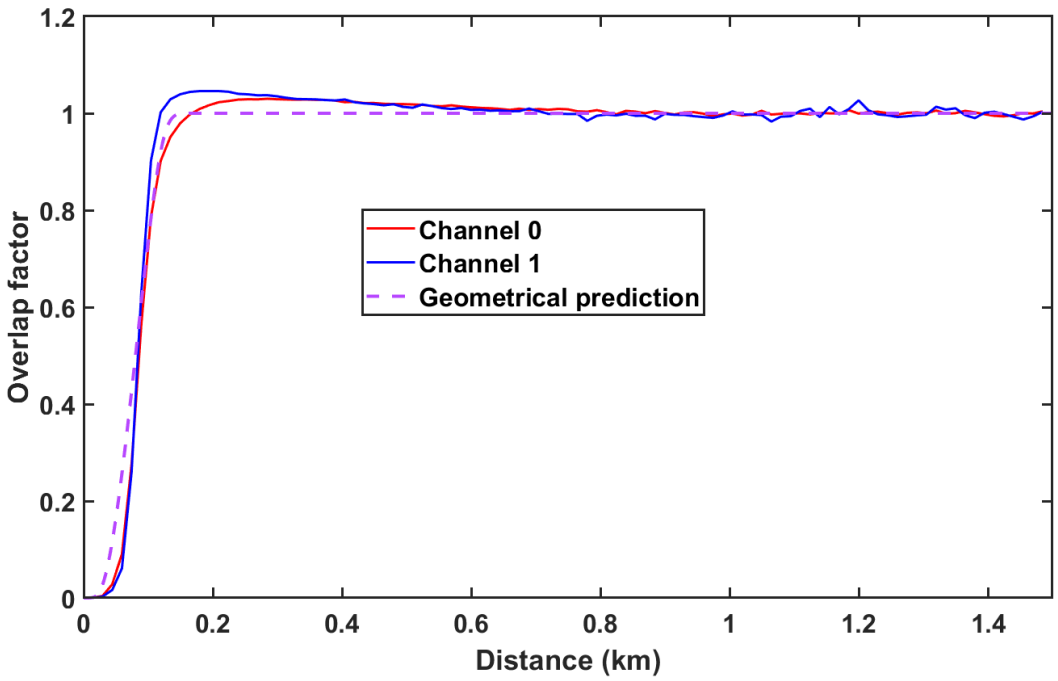

Figure 8. Overlap factor of ALiAS on board ATR-42 during EUREC^{4}A.

5.3 Level-2 and Level-3

Level-2 data are products provided for each individual lidar profile, for both cloud detection and calculation of the aerosol extinction coefficient (AEC) along the horizontal line of sight. Level-3 data result from statistics on Level-2 data.

5.3.1 Cloud products

a. Description of Level-2 cloud products

Cloud detection is applied to the lidar data acquired during the Phase 2 of the flights (rectangles). It is the basis of the Level-2 cloud dataset. For each lidar ABC profile, it uses a threshold approach as already considered for lidar measurements at nadir (Chazette et al., 2001; Shang and Chazette, 2014). The threshold is proportional to the standard deviation of the noise of the cloud-free signal during Phase 2 of a given flight. Although the coefficient of proportionality Ce is constant, the threshold varies with the distance from the aircraft owing to the decrease of the signal to noise ratio (due to the increase of the clear-sky noise) away from the aircraft. As for the aerosol products, a lidar profile is considered as being cloud-free if the logarithm of the ABC can be considered as linear with a relative error of less than 10% (cf. Section 5.3.2). The threshold is then calculated at a constant altitude (around the cloud base height, where molecular and particle scattering can be considered constant) and when the angle of the lidar line of sight with the horizontal does not exceed 3° (the mean value is 1° and the standard deviation is 0.5°). Lidar profiles acquired during ATR-42 turns are therefore excluded from the cloud Level-2 data. Figure 9a shows the evolution of the cloud-free lidar signal averaged over Phase 2, and the associated standard deviation along the horizontal line of sight for flight F05 on 28 January 2020. The standard deviation increases very rapidly with distance, just as the ABC decreases. The cloud detection was tested for different values of the coefficient C_e ranging from 1 to 8. The cloud mask turned out to be fairly insensitive to the value of C_e as long as C_e ranges from 2 and 4. To construct the Level-2 data, we choose C_e = 2.5.

Figure 9b shows that the cloud density decreases with the distance from the aircraft, especially beyond 3-4 km. This results from two different effects: as the distance from the aircraft increases, (1) the threshold for cloud detection increases (mostly because the magnitude of the noise increases, cf Figure 9a), and (2) the probability for the laser beam to be attenuated increases if multiple clouds are present along the laser line of sight. In general, one can be confident in the detection of semi-transparent cloud layers over the first 3-4 km. Beyond that, cloud detection is still possible, especially when there are no significant scattering layers (such as a dense aerosol plume) between the laser source and the cloud, but with a higher uncertainty on the detection of the cloud edges and thus the cloud depth. The presence of dense clouds that cannot be traversed by the laser beam will lead to an underestimate of the cloud cover and a negative bias on the average cloud depth. At cloud base, such clouds were only present on a few days during the campaign (e.g. F07, F12, F17, F18 and F19).

Two additional parameters are considered for the cloud detection, that can potentially be adjusted. First, we consider that two cloudy points separated by clear-sky correspond to two distinct clouds only if they are separated by a distance of at least D (in other terms, two cloudy points separated by clear-sky but distant by less than D will be considered as being part of the same cloud). Recognizing that trade-wind cumuli can be very small and close to each other (e.g. Zhao and Di Girolamo, 2007), we chose D = 30 m. Second, to avoid interpreting as a cloud a peak of the signal that would arise from noise, we impose that a cloud corresponds to a segment of adjacent cloudy points (along the line of sight) longer than a certain threshold referred to as L_{min}. The width L_{min} is more difficult to estimate. We use L_{min} = 45 m to eliminate isolated peaks (1 to 2 points only) of the lidar profiles that result from noise and strongly influence the statistics of cloud detection beyond 3-4 km. The two parameters D and L_{min} are tuneable, and the points of the cloud mask affected by these parameters are flagged in a quality indicator.

Level-2 products also include the distance d_0 beyond which the lidar signal (ABC) can be considered as undistinguishable from noise (10 consecutive points within noise after the last cloud point detected). This distance is located in a non-cloudy part of the horizontal lidar profile. It is worth noting that the ABC of clouds is more than an order of magnitude greater than that of clear air and that the lidar signal can be in the noise at d_0 while still showing the presence of a cloud at a greater distance.

Figure 11 shows an example of the detection of cloud structures on one of the lidar profiles of Flight F11 (2020-02-05 10:13:29). Two clouds are detected at a distance of about 0.9 and 3.8 km from the ATR-42. They correspond to segments composed of at least 3 successive points for which the ABC exceeds the threshold value. On the other hand, despite their ABC larger than the threshold, the segments shorter than L_{min} or the "isolated peaks" are not considered as cloudy points. The distance d_0 is reported around 4.2 km.

b. Description of Level-3 cloud products

Level-3 cloud products consist of probability distribution functions (PDFs) of cloud chords along the laser line of slight computed during Phase 2 of the flight. It is worth noting that owing to the integration/acquisition time of the lidar measurement (5 s) and the aircraft speed (100 ms^{-1}), we are unable to derive a cloud mask along the direction of aircraft motion (the minimum distance we can resolve along this direction is 500 m, which is roughly the upper bound of the cloud chords measured along the line of sight of the lidar). The cloud mask distributed in the Level-2/Level-3 datasets thus corresponds to the cloud detection done along

the line of sight of the lidar only. If clouds were homogeneously distributed within the field of view of the lidar, and perfectly detected by the lidar, similar PDFs would be inferred whatever the distance from the aircraft. Figure 11 shows the cloud width histogram derived at cloud base during flight F05 on 28 January 2020. The distribution obtained for the whole field of view of the lidar (clouds detected for horizontal distances between 0.1 to 8 km) is compared to the distribution obtained for clouds detected between 3 and 8 km from the aircraft. The good match of the two PDFs shows that, from a statistical point of view, the cloud detection is not biased with the distance from the aircraft, at least for cumulus cloud fields composed of optically thin clouds (also referred to as 'Sugar' patterns, Stevens et al. (2020)). In the case of flight F05, the mean cloud width is about 130 m with a standard deviation of 80 m.

c. The cloud detection quality indicator/flag

Level-2 cloud product also includes a binary quality indicator (or flag) coded with "1" and "0" over 6 bits, denoted Qflag. This indicator is defined in Table 4. It takes into account for each range gate along the lidar line of sight: i) the detection or not of a cloud (bit 1), ii) the aggregation or not of nearby cloud structures separated by less than D = 30 m (bit 2), iii) the detection of narrow cloud structures (cloud width along the line of sight < L_{min} = 45 m), that can be considered as signal noise and which are not considered as clouds (bit 3), iv) the vertical positioning with respect to the horizontal (Δz) of the cloud point, which depends on the angle between the line of slight and the horizontal (bits 4 and 5) and v) visual information on the level of soiling on the external face of the aircraft window crossed by the laser beam. In order to simplify its re-reading by users, the indicator is converted into real numbers in Level-2 files. Before being used, it must be converted back to binary. For example, the real number 52 corresponds to the binary number '110100'.

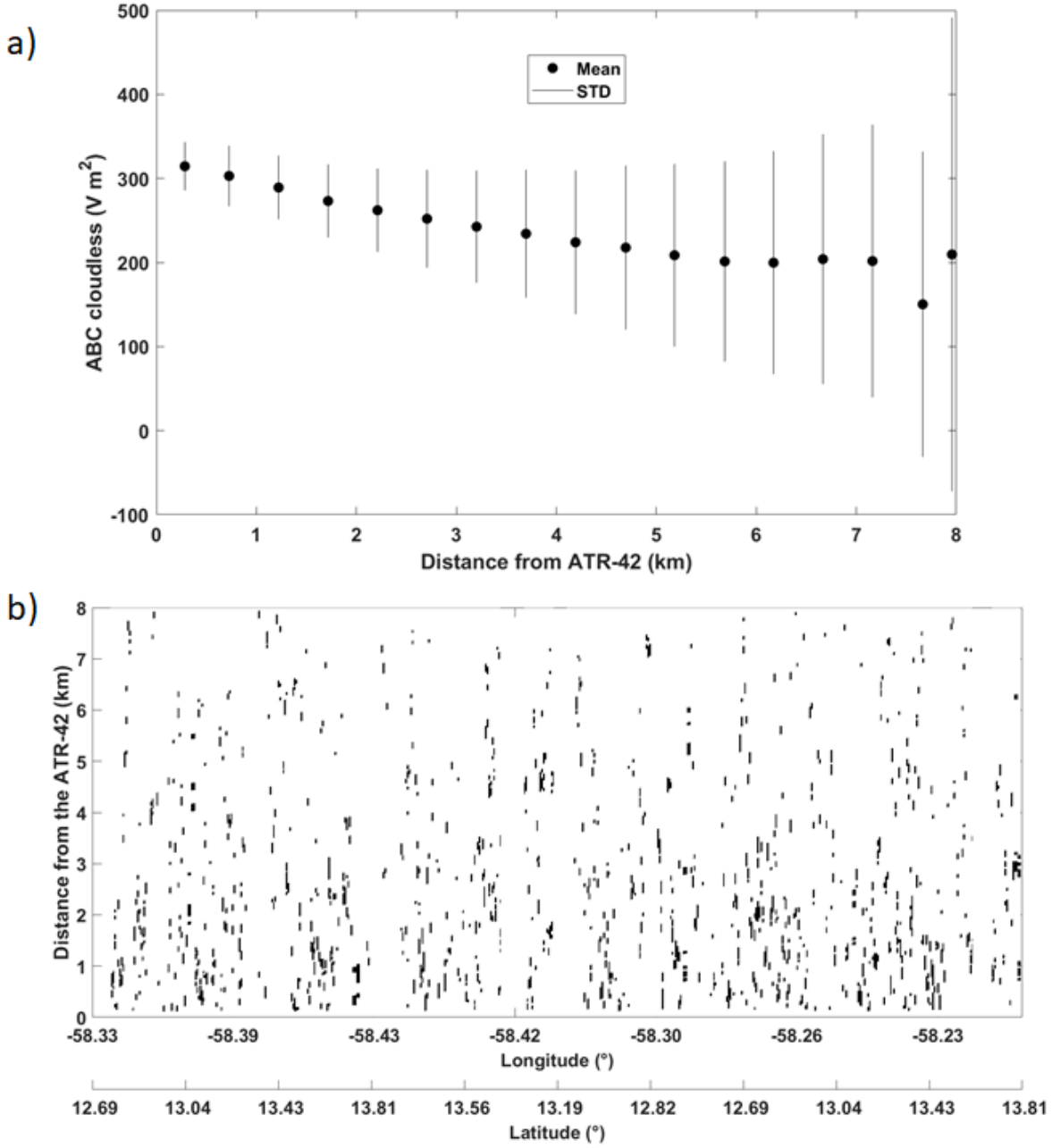

Figure 9. a) Average apparent backscatter coefficient (ABC) per 500 m distance range for all cloud-free profiles of Phase 2 for the flight F05 on 28 January 2020. The standard deviation (STD) is also reported. b) Binary cloud detection matrix derived from ALiAS measurements along the horizontal line of slight for the flight F05 on 28 January 2020, for the first rectangle of Phase 2. The cloud mask is based on a cloud detection that uses Ce = 2.5, D = 30 m and L_{min} = 45 m. It is part of Level-2 cloud products.

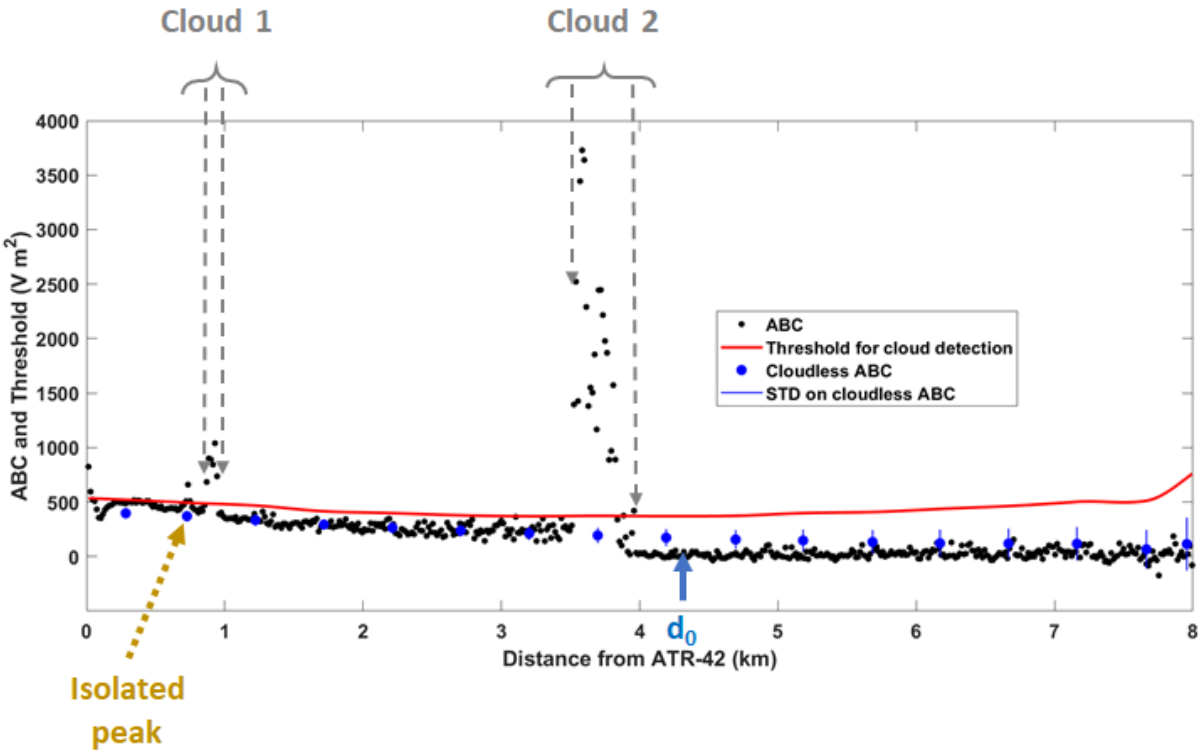

Figure 10. Illustration of the cloud detection procedure on the apparent backscatter coefficient (ABC) during the flight F11 on 5 February 2020 (10:13:29). Two clouds are detected, that correspond to successive points for which the ABC exceeds the ABC threshold 9in red). An isolated peak is not considered as a cloudy point. The distance d_0 at which the ABC can be considered as embedded in the noise is reported. The blue dotted line is the cloud-free ABC for the Phase 2 of flight F11. The standard deviation of the cloud-free ABC is also reported (blue vertical bars). At each distance, the threshold for cloud detection is defined as Ce times the threshold value.

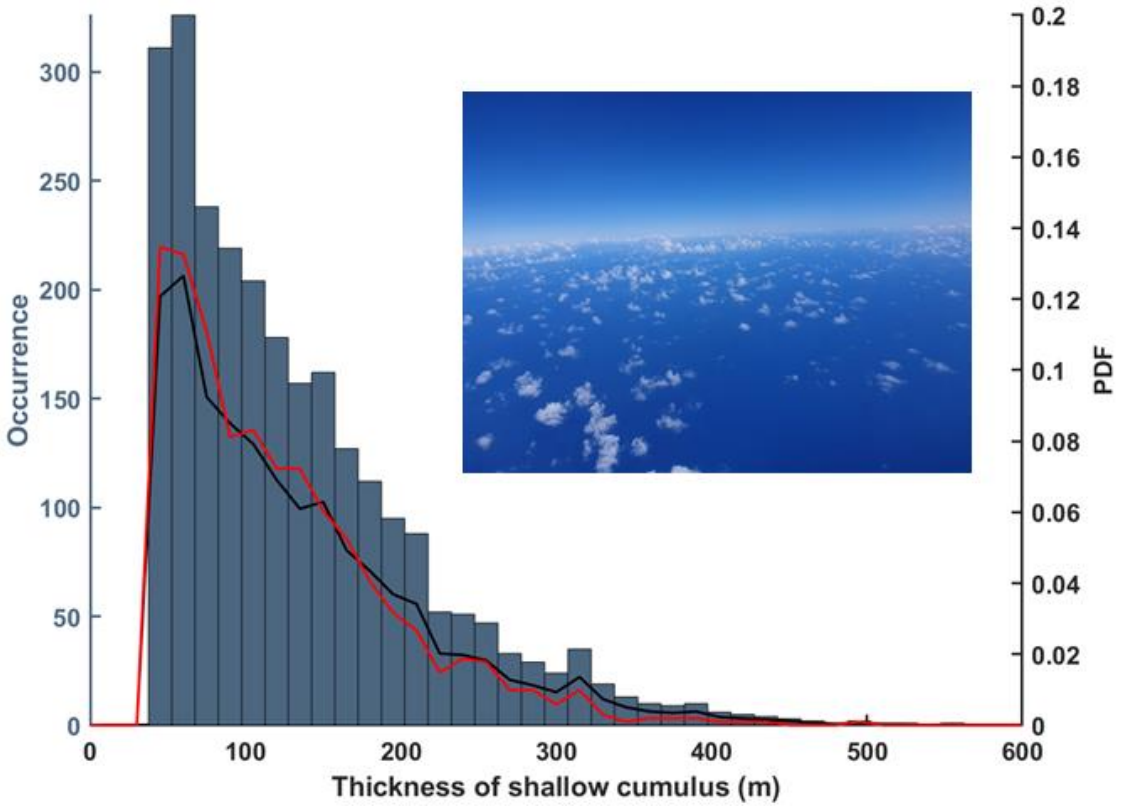

Figure 11. Number of clouds detected along the horizontal line of sight of the lidar that correspond to different cloud widths during the Phase 2 of flight F05 on 28 January 2020 (Level-3 cloud product). Also reported (right-hand side vertical axis) is the probability distribution function of cloud widths for the clouds detected at horizontal distances from the aircraft ranging from 0.1 and 8 km (black solid line) and from 3 to 8 km (red solid line). The picture illustrates the type of cloud field sampled during this flight.

Table 4. Cloud detection quality indicator (Qflag) defined on 6 bits.

Qflag	B1	B2	B3	B4	B5	B6
No cloud detection	**0**	***0***	***0***	***0***	***0***	***0/1***
Cloud detection	**1**	***0/1***	***0***	***0/1***	***0/1***	***0/1***
No agglomeration	***1***	**0**	***0***	***0/1***	***0/1***	***0/1***
Agglomeration	***1***	**1**	***0***	***0/1***	***0/1***	***0/1***
False detection	***0***	***0***	**1**	***0/1***	***0/1***	***0/1***
Δz < 100 m	***1***	***0/1***	***0***	**0**	**0**	***0/1***
100 < Δz < 200	***1***	***0/1***	***0***	**0**	**1**	***0/1***
200 < Δz < 300	***1***	***0/1***	***0***	**1**	**0**	***0/1***
300 < Δz	***1***	***0/1***	***0***	**1**	**1**	***0/1***
Clear window	***1***	***0/1***	***0***	***0/1***	***0/1***	**0**
Clogged window	***1***	***0/1***	***0***	***0/1***	***0/1***	**1**

5.3.2 Aerosol products

The AECs are the second Level-2&3 products derived from the horizontal line of sight of the ALiAS lidar. The Barbados area is a region where a very wide variety of aerosols can be found. The main ones are marine aerosols to which can be added terrigenous aerosols and even biomass burning aerosols. It has been known for decades that these terrigenous aerosols mainly originate from West Africa and that their concentration over Barbados is marked by a strong seasonality (Prospero, 1968) with a maximum during the boreal summer. Dust aerosols are carried across the North Atlantic by Trade Winds (Trapp et al., 2010) and their concentration depends on the meteorological conditions over both Africa and the tropical North Atlantic Ocean. Main studies on desert dust aerosols have been conducted on the basis of dust events in Barbados whose sources were located more than 5000 km away over the Western Sahara (e.g. Haarig et al., 2017; Trapp et al., 2010). Although this type of event occurs rarely in winter, during several flights, we observed strong AEC values associated with a significant depolarization signature. Terrigenous aerosols were actually observed for about half of the ATR flights during EUREC^{4}A (Table 5).

The process for determining the AEC from horizontal lidar measurements was first described in Chazette et al. (2007). The horizontal configuration allows to directly measure the AEC, by measuring the exponential attenuation of the signal, provided the atmosphere is sufficiently homogeneous over a few kilometers, i.e. in clear-sky air ($\alpha_n(\mathrm{z}) = 0$). Under the conditions of the field experiment, in order to limit the effect of both the signal noise and the overlap factor, the calculation of the AEC is performed by linear regression on $Ln(ABC(x,z))$ in the range from 0.2 to 1 km away from the aircraft. The slope of the regression line is equal to $-2\alpha_a(z)$ and is given by (Chazette, 2020)

$$\alpha_a(z) = -\frac{1}{2}\frac{\partial Ln(ABC(x,z))}{\partial x} \quad (6)$$

Only AECs associated with a relative regression error of less than 10% are retained. This avoids cloud-contaminated profiles in the regression range. The determination of the AEC is direct, without any hypothesis on the nature of the aerosol. In order to limit the effect related to a deviation from the horizontal, profiles with angles to the horizontal greater than 10° are removed. It should be noted that an angular deviation of 15° induces an error of 0.01 km^{-1} on the AEC. The mean VDR ($\overline{VDR}(z) = {}^{1}/_{0.8}\int_{0.2}^{1} VDR(x,z)\cdot dx$) is also calculated over the same distance range as the AEC and is part of the aerosol Level-2 data.

Level-3 aerosol data consists of average AEC and VDR profiles calculated over each entire flight. Standard deviations on the AEC and VDR are associated with them. It was chosen to discretize the atmosphere with altitude steps of 100 m for these mean profiles.

Figure 12 shows the evolution of the AEC and VDR over the entire Flight F07 on 31 January 2020 (Level-2 products). The aerosol loading is significant during Phase 2 of the flight, where cloud detection is performed. AECs of ~0.3 km^{-1} and even higher are observed. These values should be compared to the background values which are well below 0.1 km^{-1}. VDRs are also high, above 2%, which is the signature of terrigenous particles in the atmosphere (e.g. Flamant et al., 2018).

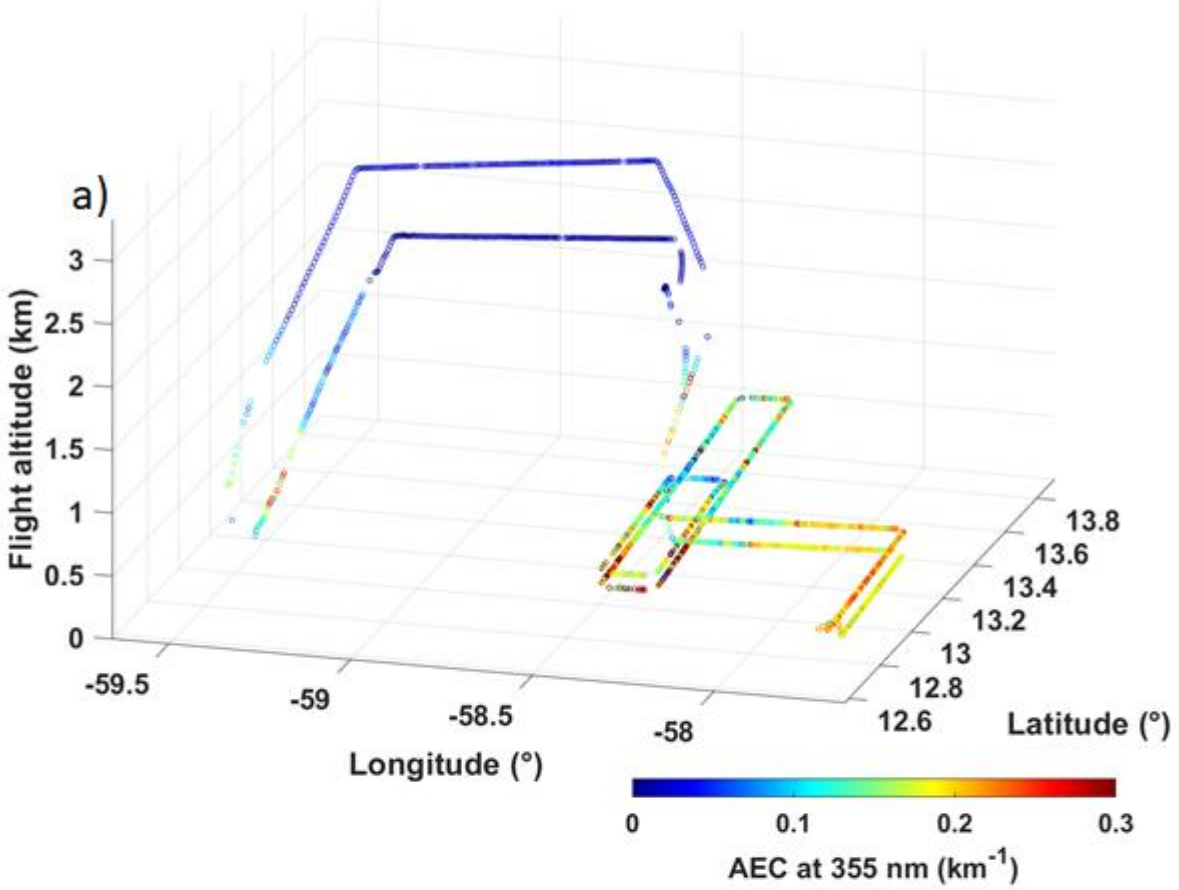
a)
Flight altitude (km)
3
2.5
2
1.5
1
0.5
0
-59.5
-59
-58.5
-58
Longitude (°)
13.8
13.6
13.4
13.2
13
12.8
12.6
Latitude (°)
0
0.1
0.2
0.3
AEC at 355 nm (km-1)

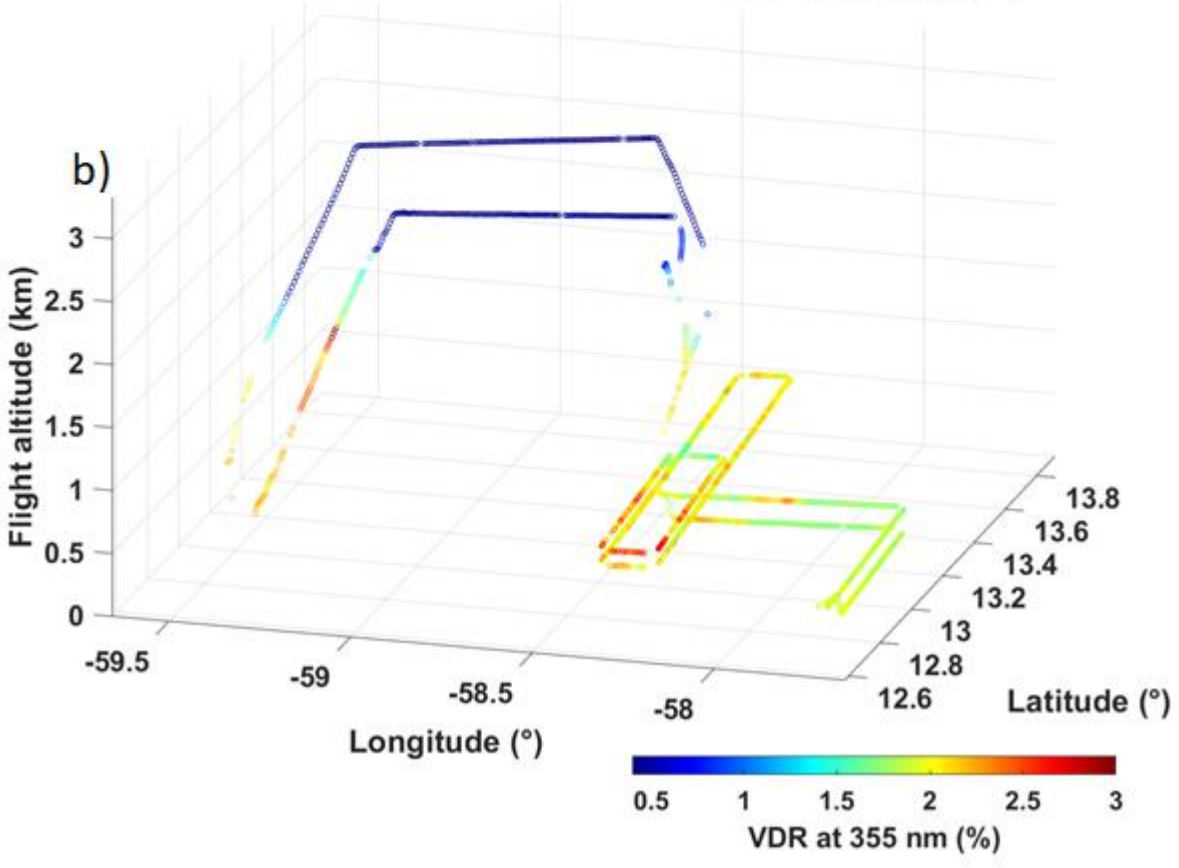
b)
Flight altitude (km)
3
2.5
2
1.5
1
0.5
0
-59.5
-59
-58.5
-58
Longitude (°)
13.8
13.6
13.4
13.2
13
12.8
12.6
Latitude (°)
0.5
1
1.5
2
2.5
3
VDR at 355 nm (%)

Figure 12. Aerosol optical properties derived from ALiAS measurements along the horizontal line of slight on 31 January 2020 (flight F07): a) aerosol extinction coefficient (AEC) and b) volume depolarisation ratio (VDR) which correspond to level 2 aerosol products.

6 Available data

6.1 Overview of available data

The ALiAS system has been successfully operated during the 20 flights of the EUREC^{4}A field campaign from 23 January to 13 February 2020. The related dataset is summarized in Table 5. Flights where the lidar sampled a significant amount of clouds ($\gtrsim$ 1000) are highlighted in bold font. The mean value of the AEC and its standard deviation informs on the amount of aerosols encountered during Phase 2 of each flight (Figure 3). Note that Phase 2 was not carried out during the test flight on 23 January 2020.

Table 5: General flight characteristics of ATR-42 when operating ALiAS. The mean, standard deviation and maximum value of the aerosol extinction coefficient (AEC) and the volume depolarization ratio (VDR) for each Phase 2 (Figure 3) of each flight are reported. The flights in bold font are those associated with the detection of many clouds. The comment " Strong presence of dusts" corresponds to VDR > 2% and the comment "Presence of dusts" corresponds to 1% < VDR < 2%. Flights with a reduced detection range due to window clogging by dusts and/or sea salt aerosols are indicated by "X".

Flight	Date (dd/mm)	Start and end time (UTC, HHMM)	Altitude range (km)	**AEC ± std (km^{-1})** max(AEC) ***VDR ± std (%)*** *max(VDR)* during Phase 2	Comment
F01	23/01	1900-2100	0.06 -3.5	Test flight	Test flight
F02	**25/01**	**1330-1745**	**0.3-4.8**	**0.03±0.03** 0.24 ***0.3±0.1*** *1.1*	-
F03	**26/01**	**1200-1600**	**0.06-4.5**	**No aerosol data**	**Modified field of view**
F04	26/01	1700-2100	0.06-2.6	**0.02±0.02** 0.1 ***0.8±0.1*** *0.9*	-
F05	**28/01**	**1615-2050**	**0.4-3.2**	**0.06±0.04** 0.3 ***0.5±0.1*** *2.9*	**Presence of dust**
F06	**30/01**	**2030-0045**	**0.3-3.2**	**0.09±0.10** 0.5 ***1.4±0.5*** *3.2*	**Presence of dust**

F07	31/01	1500-1845	0.3-3.25	**0.14±0.06** 0.6 ***2.1±0.2*** *2.7*	Strong presence of dust
F08	31/01	1945-2400	0.3-3.25	**0.20±0.08** 0.7 ***2.2±0.3*** *3.2*	Strong presence of dust X
F09	02/02	1145-1545	0.3-3.25	**0.14±0.06** 0.5 ***3.0±0.6*** *4.6*	Strong presence of dust
F10	02/02	1645-2100	0.06-3.25	**0.16±0.04** 0.4 ***2.7±0.4*** *3.7*	Strong presence of dust
F11	**05/02**	**0845-1300**	**0.06-3.25**	**0.13±0.08** 0.87 ***1.4±0.1*** *2.1*	**Presence of dust**
F12	**05/02**	**1345-1815**	**0.06-3.25**	0.13±0.07 0.53 *1.4±0.2* *1.8*	**Presence of dust**
F13	**07/02**	**1130-1545**	**0.06-3.25**	**0.06±0.04** 0.36 ***0.4±0.3*** *2.1*	-
F14	07/02	1700-2145	0.06-3.25	**0.04±0.04** 0.27 ***0.3±0.2*** 0.7	-
F15	09/02	0445-0900	0.06-4.4	**0.18±0.10** 0.53 ***0.6±0.1*** *0.9*	X
F16	09/02	1400-1815	0.06-4.5	**0.18±0.07** 0.55 ***0.9±0.2*** *1.5*	X
F17	11/02	0600-1030	0.25-4.5	**0.15±0.16** 1.2 ***0.7±0.1*** *1.1*	-
F18	11/02	1130-1600	0.06-4	**0.19±0.13** 0.92 ***1.0±0.2*** 1.4	Presence of dust X
F19	**13/02**	**0730-1145**	**0.06-3.25**	**0.09±0.08** 0.39	-

				0.6±0.3 *2.3*	
F20	13/02	1300-1730	0.06-2.5	**0.05±0.04** 0.37 ***0.6±0.4*** *2.1*	-

6.2 Files format

For each flight, data are available within the database as NetCDF files (version 4) for the four levels of processing described in section 5. The Level-1 NetCDF file contains raw data recorded during the whole duration of the flight. It contains all the scalar and time-dependent parameters needed to properly process the signal recorded by each lidar channel. The Level-1.5 NetCDF file contains pre-processed lidar profiles of ABC and VDR along the lidar line of sight, as a function of time. Also provided are the distance from the aircraft (time dependent) and flight attitude, localization and altitude useful for data geo-localization.

Level-2 and Level-3 are concatenated into one single NetCDF file, separately for clouds and aerosols products. The aerosol Level-2&3 NetCDF file contains cloud-free AEC individual values with the corresponding altitude, time, and geo-localization parameters, and the mean vertical profile of AEC within the altitude range of the flight, respectively. The cloud Level-2&3 NetCDF file contains the ABC used in the detection algorithm of clouds, a binary cloud detection array (cloud mask) and a quality flag array. All-three are given as a function of the distance from the aircraft and are restricted to the rectangle flight patterns of Phase 2, and profiles with roll/pitch angles close to 0°. The Level-2&3 NetCDF file also includes the probability density functions (PDF) of the cloud widths encountered during the Phase 2 of the flight. PDFs are computed along the horizontal lines of slight for distances ranging between 0.1 and 8 km, and between 3 and 8 km, to check for the consistency of measurements in the near and far-field.

The entire dataset is published in open access on the AERIS database (https://en.aeris-data.fr/). The digital object identifier (DOI) for Level-1 and Level-1.5 data is 10.25326/57 (https://doi.org/10.25326/57; Chazette et al., 2020c). For Level-2&3 data, it is 10.25326/58 for the cloud products (https://doi.org/10.25326/58; Chazette et al., 2020b), and 10.25326/59 for the aerosol products (https://doi.org/10.25326/59; Chazette et al., 2020a). The typical sizes of the different NetCDF files are: i) ~ 195-420 Mo for Level-1 data, ii) ~11-29 Mo for Level-1.5 data, iii) ~4-18 Mo for Level-2&3 cloud products, and iv) ~60-190 Ko for Level-2&3 aerosol products.

7 Summary

An airborne sidewards-staring lidar was implemented on board the ATR-42 for the EUREC^{4}A field campaign. Twenty flights were conducted from 23 January to 13 February 2020 over the west Atlantic Ocean tropical region, off the coast of Barbados. The horizontal line of sight of the lidar allowed us to characterize horizontal fields of shallow cumuli with a much better sampling than would have been the case with nadir or zenith measurements. This new dataset will make it possible to analyse the macroscopic properties of shallow cumuli near cloud base for a range of meteorological conditions and mesoscale organizations. It will also offer a baseline measurement to assess the value of future space-borne missions as the forthcoming Earth Clouds, Aerosols and Radiation Explorer mission (EarthCARE, Illingworth et al., 2015) and to evaluate the realism of the new generation climate models. Aerosol optical parameters were also derived; biomass burning and dust aerosol plumes were present during the field campaign. The data has been classified according to the level of numerical processing applied: i) Level 1 data is the raw horizontal lidar profiles, ii) Level-1.5 data is the calibrated lidar profiles corrected from system characteristics, iii) Level-2 data is the geophysical parameters directly derived from the individual profiles and iv) Level-3 data is the synthesis of these parameters. Level-2 and Level-3 data have been combined in the same NetCDF files. All these data are available on the AERIS database (https://en.aeris-data.fr/).

Author contributions. Patrick Chazette participated to the field experiment on board ATR-42, analyzed the data, developed the algorithms for the Level-1.5, 2 and 3 datasets, and wrote the paper; Julien Totems, Alexandre Baron and Cyrille Flamant participated to the field experiment on board ATR-42 and contributed to the paper writing; Sandrine Bony coordinated the project, participated to the field experiment on board ATR-42 and contributed to the paper writing.

Competing interests. The authors declare that they have no conflict of interest.

Acknowledgements. The idea of trying horizontal lidar measurements to characterize clouds at cloud base was suggested to us by Bjorn Stevens at the outset of the EUREC^{4}A project. The authors gratefully acknowledge Jean-Christophe Canonici, Jean-Christophe Desbios, Thierry Perrin, Laurent Guiraud and all the Technicians, Engineers, Pilots and Director from SAFIRE, the French facility for airborne research (http://www.safire.fr), and Airplane Delivery, for making the preparation of the ATR and the EUREC^{4}A airborne operations possible. We thank the Caribbean Regional Security System (RSS) for hosting the ATR and the ATR team in Barbados during the experiment, Dr David Farrell and the Caribbean Institute for Meteorology

and Hydrology (CIMH) for their logistical and administrative support, the Department of Civil Aviation in Barbados and Andrea Hausold (from DLR), for their help and support of airborne operations. The authors also thank AERIS for their support during the campaign and for managing the EUREC^{4}A database. The EUREC^{4}A project was supported by the European Research Council (ERC) under the European Union's Horizon 2020 research and innovation programme (Grant Agreement No. 694768), with some additional support from by the French Space Agency CNES through the EECLAT project. The authors are thankful to the three anonymous referees whose comments helped improve the overall quality of the paper.

References

Berthier, S., Pelon, J., Chazette, P., Couvert, P., Sèze, G., Bréon, F.-M., Laland, M., Winker, D. and Pain, T.: Cloud statistics from spaceborne backscatter lidar data analysis, in European Space Agency, (Special Publication) ESA SP, vol. 2., 2004.

Bony, S. and Dufresne, J. L.: Marine boundary layer clouds at the heart of tropical cloud feedback uncertainties in climate models, Geophys. Res. Lett., 32(20), 1–4, doi:10.1029/2005GL023851, 2005.

Bony, S., Stevens, B., Ament, F., Bigorre, S., Chazette, P., Crewell, S., Delanoë, J., Emanuel, K., Farrell, D., Flamant, C., Gross, S., Hirsch, L., Karstensen, J., Mayer, B., Nuijens, L., Ruppert, J. H., Sandu, I., Siebesma, P., Speich, S., Szczap, F., Totems, J., Vogel, R., Wendisch, M. and Wirth, M.: EUREC^{4}A: A Field Campaign to Elucidate the Couplings Between Clouds, Convection and Circulation, Surv. Geophys., doi:10.1007/s10712-017-9428-0, 2017.

Bony, S., Schulz, H., Vial, J. and Stevens, B.: Sugar, Gravel, Fish, and Flowers: Dependence of Mesoscale Patterns of Trade-Wind Clouds on Environmental Conditions, Geophys. Res. Lett., 47(7), 1–12, doi:10.1029/2019GL085988, 2020.

Brient, F., Schneider, T., Tan, Z., Bony, S., Qu, X. and Hall, A.: Shallowness of tropical low clouds as a predictor of climate models' response to warming, Clim. Dyn., 47(1), 433–449, doi:10.1007/s00382-015-2846-0, 2016.

Chazette, P.: Aerosol optical properties as observed from an ultralight aircraft over the Strait of Gibraltar, Atmos. Meas. Tech. Discuss., 2011(August 2011), 1–24, doi:10.5194/amt-2020-131, 2020.

Chazette, P., Pelon, J. and Mégie, G.: Determination by spaceborne backscatter lidar of the structural parameters of atmospheric scattering layers., Appl. Opt., 40(21), 3428–3440, doi:10.1364/AO.40.003428, 2001.

Chazette, P., Sanak, J. and Dulac, F.: New approach for aerosol profiling with a lidar onboard an ultralight aircraft: application to the African Monsoon Multidisciplinary Analysis., Environ. Sci. Technol., 41(24), 8335–8341, doi:10.1021/es070343y, 2007.

Chazette, P., Bocquet, M., Royer, P., Winiarek, V., Raut, J. C., Labazuy, P., Gouhier, M., Lardier, M. and Cariou, J. P.: Eyjafjallajökull ash concentrations derived from both lidar and modeling, J. Geophys. Res. Atmos., 117, doi:10.1029/2011JD015755, 2012a.

Chazette, P., Dabas, a., Sanak, J., Lardier, M. and Royer, P.: French airborne lidar measurements for Eyjafjallajökull ash plume survey, Atmos. Chem. Phys., 12(15), 7059–7072, doi:10.5194/acp-12-7059-2012, 2012b.

Chazette, P., Totems, J., Hespel, L. and Bailly, J. S.: Principle and Physics of the LiDAR Measurement, in Optical Remote Sensing of Land Surface: Techniques and Methods, pp. 201–247., 2016.

Chazette, P., Raut, J. C. and Totems, J.: Springtime aerosol load as observed from ground-based and airborne lidars over northern Norway, Atmos. Chem. Phys., 18(17), 13075–13095, doi:10.5194/acp-18-13075-2018, 2018.

Chazette, P., Totems, J., Baron, A., Flamant, C. and Bony, S.: EUREC4A – ATR-42 – Lidar ALiAS – Level 2 & 3 aerosol products, AERIS data Cent., doi:10.25326/59, 2020a.

Chazette, P., Totems, J., Baron, A., Flamant, C. and Bony, S.: EUREC4A ATR-42 Lidar ALiAS – Level 2 & 3 cloud products, AERIS data Cent., doi:10.25326/58, 2020b.

Chazette, P., Totems, J., Baron, A., Flamant, C. and Bony, S.: EUREC4A ATR-42 Lidar ALiAS – Levels 1 & 1.5, AERIS data Cent., doi:10.25326/57, 2020c.

Collis, R. T. H. and Russel, P. B.: Laser Monitoring of the Atmosphere, edited by E. D. Hinkley, Springer Berlin Heidelberg, Berlin, Heidelberg., 1976.

Flamant, C., Deroubaix, A., Chazette, P., Brito, J., Gaetani, M., Knippertz, P., Fink, A. H., de Coetlogon, G., Menut, L., Colomb, A., Denjean, C., Meynadier, R., Rosenberg, P., Dupuy, R., Schwarzenboeck, A. and Totems, J.: Aerosol distribution in the northern Gulf of Guinea: local anthropogenic sources, long-range transport and the role of coastal shallow circulations, Atmos. Chem. Phys. Discuss., 18(16), 1–71, doi:10.5194/acp-2018-346, 2018.

Haarig, M., Ansmann, A., Althausen, D., Klepel, A., Groß, S., Freudenthaler, V., Toledano, C., Mamouri, R. E., Farrell, D. A., Prescod, D. A., Marinou, E., Burton, S. P., Gasteiger, J., Engelmann, R. and Baars, H.: Triple-wavelength depolarization-ratio profiling of Saharan dust over Barbados during SALTRACE in 2013 and 2014, Atmos. Chem. Phys., 17(17), 10767–10794, doi:10.5194/acp-17-10767-2017, 2017.

Illingworth, A. J., Barker, H. W., Beljaars, A., Ceccaldi, M., Chepfer, H., Clerbaux, N., Cole, J., Delanoë, J., Domenech, C., Donovan, D. P., Fukuda, S., Hirakata, M., Hogan, R. J., Huenerbein, A., Kollias, P., Kubota, T., Nakajima, T. Y., Nakajima, T. Y., Nishizawa, T., Ohno, Y., Okamoto, H., Oki, R., Sato, K., Satoh, M., Shephard, M. W., Velázquez-Blázquez, A., Wandinger, U., Wehr, T. and Van Zadelhoff, G. J.: The earthcare satellite : The next step forward in global measurements of clouds, aerosols, precipitation, and radiation, Bull. Am. Meteorol. Soc., 96(8), 1311–1332, doi:10.1175/BAMS-D-12-00227.1, 2015.

Johnson, B. T. T., Heese, B., McFarlane, S. A. a., Chazette, P., Jones, A. and Bellouin, N.: Vertical distribution and radiative effects of mineral dust and biomass burning aerosol over West Africa during DABEX, J. Geophys. Res., 113(23), 1–16, doi:10.1029/2008JD009848, 2008.

Liou, K.-N. and Schotland, R. M.: Multiple Backscattering and Depolarization from Water Clouds for a Pulsed Lidar System, J. Atmos. Sci., 28(5), 772–784, doi:10.1175/1520-0469(1971)028<0772:mbadfw>2.0.co;2, 1971.

Medeiros, B., Stevens, B. and Bony, S.: Using aquaplanets to understand the robust responses of comprehensive climate models to forcing, Clim. Dyn., 44(7–8), 1957–1977, doi:10.1007/s00382-014-2138-0, 2015.

Norris, J. R.: Low cloud type over the ocean from surface observations. Part II: Geographical and seasonal variations, J. Clim., 11(3), 383–403, doi:10.1175/1520-0442(1998)011<0383:LCTOTO>2.0.CO;2, 1998.

Nuijens, L. and Siebesma, A. P.: Boundary Layer Clouds and Convection over Subtropical Oceans in our Current and in a Warmer Climate, Curr. Clim. Chang. Reports, 5(2), 80–94, doi:10.1007/s40641-019-00126-x, 2019.

Palm, S. P., Benedetti, A. and Spinhirne, J.: Validation of ECMWF global forecast model parameters using GLAS atmospheric channel measurements, Geophys. Res. Lett., 32(22), n/a-n/a, doi:10.1029/2005GL023535, 2005.

Pierrehumbert, R. T.: Thermostats, radiator fins, and the local runaway greenhouse, J. Atmos. Sci., 52(10), 1784–1806, 1995.

Prospero, J. M.: atmospheric dust studies on Barbados, Bull. Am. Meteorol. Soc., 49(6), 645–

652, doi:10.1175/1520-0477-49.6.645, 1968.
Redelsperger, J. L., Thorncroft, C. D., Diedhiou, A., Lebel, T., Parker, D. J. and Polcher, J.: African Monsoon Multidisciplinary Analysis: An international research project and field campaign, Bull. Am. Meteorol. Soc., 87(12), 1739–1746, doi:10.1175/BAMS-87-12-1739, 2006.
Shang, X. and Chazette, P.: Interest of a Full-Waveform Flown UV Lidar to Derive Forest Vertical Structures and Aboveground Carbon, Forests, 5(6), 1454–1480, doi:10.3390/f5061454, 2014.
Shang, X. and Chazette, P.: End-to-End Simulation for a Forest-Dedicated Full-Waveform Lidar onboard a Satellite Initialized from UV Airborne Lidar Experiments, Remote Sens., 7(5), 5222–5255, doi:10.3390/rs70505222, 2015.
Spark, M. and Cottis, M.: Pressure-induced optical distorsion in laser windows, Appl. Opt., 44(2), 787–794, 1973.
Spinhirne, J. D., Hansen, M. Z. and Caudill, L. O.: Cloud top remote sensing by airborne lidar, Appl. Opt., 21(9), 1564, doi:10.1364/ao.21.001564, 1982.
Spinhirne, J. D., Palm, S. P., Hlavka, D. L., Hart, W. D. and Welton, E. J.: Global aerosol distribution from the GLAS polar orbiting lidar instrument, IEEE Work. Remote Sens. Atmos. Aerosols, 2005., doi:10.1109/AERSOL.2005.1494140, 2005.
Stevens, B., Ament, F., Bony, S., Crewell, S., Ewald, F., Gross, S., Hansen, A., Hirsch, L., Jacob, M., Kölling, T., Konow, H., Mayer, B., Wendisch, M., Wirth, M., Wolf, K., Bakan, S., Bauer-Pfundstein, M., Brueck, M., Delanoë, J., Ehrlich, A., Farrell, D., Forde, M., Gödde, F., Grob, H., Hagen, M., Jäkel, E., Jansen, F., Klepp, C., Klingebiel, M., Mech, M., Peters, G., Rapp, M., Wing, A. A. and Zinner, T.: A high-altitude long-range aircraft configured as a cloud observatory the narval expeditions, Bull. Am. Meteorol. Soc., 100(6), 1061–1077, doi:10.1175/BAMS-D-18-0198.1, 2019.
Stevens, B., Bony, S., Brogniez, H., Hentgen, L., Hohenegger, C., Kiemle, C., L'Ecuyer, T. S., Naumann, A. K., Schulz, H., Siebesma, P. A., Vial, J., Winker, D. M. and Zuidema, P.: Sugar, gravel, fish and flowers: Mesoscale cloud patterns in the trade winds, Q. J. R. Meteorol. Soc., 146(726), 141–152, doi:10.1002/qj.3662, 2020.
Trapp, J. M., Millero, F. J. and Prospero, J. M.: Temporal variability of the elemental composition of African dust measured in trade wind aerosols at Barbados and Miami, Mar. Chem., 120(1–4), 71–82, doi:10.1016/j.marchem.2008.10.004, 2010.
Vial, J., Bony, S., Stevens, B. and Vogel, R.: Mechanisms and Model Diversity of Trade-Wind Shallow Cumulus Cloud Feedbacks: A Review, pp. 159–181, Springer, Cham., 2017.
Winker, D. M., Pelon, J., Mccormick, M. P., Pierre, U. and Jussieu, P.: The CALIPSO mission : Spaceborne lidar for observation of aerosols and clouds, Proc. SPIE vol. 4893, 4893, 1–11, doi:10.1117/12.466539, 2003.
Yorks, J. E., McGill, M. J., Palm, S. P., Hlavka, D. L., Selmer, P. A., Nowottnick, E. P., Vaughan, M. A., Rodier, S. D. and Hart, W. D.: An overview of the CATS level 1 processing algorithms and data products, Geophys. Res. Lett., 43(9), 4632–4639, doi:10.1002/2016GL068006, 2016.
Zhao, G. and Di Girolamo, L.: Statistics on the macrophysical properties of trade wind cumuli over the tropical western Atlantic, J. Geophys. Res. Atmos., 112(10), doi:10.1029/2006JD007371, 2007.